A SURVEY OF LOCAL GROUP GALAXIES CURRENTLY FORMING STARS. I. *UBVRI* PHOTOMETRY OF STARS IN M31 AND M33[1]

Philip Massey,[2,3] K. A. G. Olsen,[4] Paul W. Hodge,[5] Shay B. Strong,[2,6] George H. Jacoby,[7]
Wayne Schlingman,[8] and R. C. Smith[4]

ABSTRACT

We present *UBVRI* photometry obtained from Mosaic images of M31 and M33 using the Kitt Peak National Observatory 4 m telescope. We describe our data reduction and automated photometry techniques in some detail, as we will shortly perform a similar analysis of other Local Group galaxies. The present study covered $2.2 \deg^2$ along the major axis of M31 and $0.8 \deg^2$ on M33, chosen so as to include all of the regions currently active in forming massive stars. We calibrated our data using photometry from the Lowell 1.1 m telescope, and this external method resulted in millimagnitude differences in the photometry of overlapping fields, providing some assurance that our photometry is reliable. The final catalog contains 371,781 and 146,622 stars in M31 and M33, respectively, where every star has a counterpart in (at least) the B, V, and R passbands. Our survey goes deep enough to achieve 1%–2% photometry at 21 mag (corresponding to stars more massive than $20\,M_\odot$) and achieves <10% errors at $U \sim B \sim V \sim R \sim I \sim$ 23 mag. Although our typical seeing was only modest ($0\farcs8$–$1\farcs4$, with median $1\farcs0$) by some standards, we find excellent correspondence between our catalog sources and those we see in our *Hubble Space Telescope* ACS data for OB48, a crowded region in M31. We compare our final photometry with that of others and find good agreement with the CCD catalog of M31 stars by Magnier et al., although our study covers twice the area and goes about 2 mag deeper. There is also excellent agreement with the CCD "DIRECT" surveys of M31 and M33. The photographic studies of others fare less well, particularly at the faint end in *V*, where accurate background subtraction is needed for good photometry. We provide cross-references to the stars confirmed as members by spectroscopy and compare the locations of these to the complete set in color-magnitude diagrams. While follow-up spectroscopy is needed for many projects, we demonstrate the success of our photometry in being able to distinguish M31/M33 members from foreground Galactic stars. Finally, we present the results of a single night of spectroscopy on the WIYN 3.5 m telescope, examining the brightest likely members of M31. The spectra identify 34 newly confirmed members, including B–A supergiants, the earliest O star known in M31, and two new luminous blue variable candidates whose spectra are similar to that of P Cygni.

Key words: catalogs — galaxies: individual (M31, M33) — galaxies: stellar content — stars: early-type — supergiants — surveys

Online material: machine-readable tables

1. INTRODUCTION

The galaxies of the Local Group serve as our astrophysical laboratories for studying the effects that metallicity and other environmental factors have on star formation and massive star evolution. The advent of 4 m class telescopes and single-object spectrographs in the 1970s heralded in an era of such studies in the Magellanic Clouds, where even the modest change in metallicity (a factor of 4 from the SMC to the Milky Way) resulted in some revealing differences in the characteristics of the massive star populations, such as the distribution of spectral subtypes of Wolf-Rayet stars and red supergiants (RSGs), as well as a factor of 100 difference in their relative numbers. These differences are believed to be due to the effect that metallicity has on the mass-loss rates of massive stars and the subsequent large effect on stellar evolution. (For a recent review, see Massey [2003].) The observed ratios can be used to test and "fine-tune" stellar evolution theory (see Meynet & Maeder 2005), and so it is important for such measurements to be extended to as low and as high metallicities as possible. With the introduction of multiobject spectrographs on larger aperture telescopes (GMOS on Gemini and DEIMOS on Keck), it is now possible to extend such studies to the more distant members of the Local Group, where the galaxies forming stars span a range of 20 in metallicity (from WLM to M31; see Table 1 of Massey 2003).

Such spectroscopic studies require the knowledge of an appropriate sample of stars to observe. We became aware of the need for a comprehensive survey of the resolved stellar content of nearby galaxies in support of our own research; we realized, however, that an additional strength of this study would be the uses that other researchers could make of such data. We took advantage of the NOAO Survey Program to use the Mosaic CCD cameras on

---

FIG. 1.—M31 Mosaic fields. We show here the 10 fields (numbered from upper left to lower right) that we used to cover the star formation regions of M31. A slight (several ADU) problem with the flatness of the stacked image of field 2 (*upper left*) results in the slightly different color; the problem did not affect our photometry, which relies on local sky determination. Each Mosaic field is roughly $36' \times 36'$ in size. The coverage of M31 was designed to go beyond the OB associations identified by van den Bergh (1964).

FIG. 2.—M33 Mosaic fields. We show here the three fields (north, center, and south) that we used to cover the star-forming regions of M33. Our coverage extends well beyond the OB associations identified by Humphreys & Sandage (1980).

the Kitt Peak National Observatory (KPNO) and Cerro Tololo Inter-American Observatory (CTIO) 4 m telescopes to image the Local Group galaxies currently actively forming stars. Our Local Group Galaxies Survey (LGGS) project imaged the nearby spiral galaxies M31 in 10 fields, and M33 in three fields, as well as the dwarf irregular galaxies NGC 6822, WLM, IC 10, the Phoenix Dwarf, Pegasus, Sextans A, and Sextans B, each in a single field. (The need to complete M31 and M33 precluded the inclusion of IC 1613, which is located at a similar right ascension, but we hope someday to correct the omission.) The survey includes *UBVRI* data, as well as images through narrowband (50–80 Å) filters centered on Hα, [O III] λ5007, and [S II] λ6713, 6731. Our goal was to obtain uniform large-area coverage of the star-forming regions in these galaxies, with broadband photometry good to 1%–2% for massive stars ($\geq$20 $M_\odot$). The data would be taken under good, but not always excellent, seeing conditions ($<$1″0–1″2). These data could be supplemented by WFPC2/ACS images with the *Hubble Space Telescope* (*HST*) or by adaptive optics for higher resolution studies of small regions, but our survey would provide uniform coverage of the entire galaxies. The broadband photometry would be used to characterize the populations of massive stars in these galaxies. By itself, it would separate RSGs from foreground dwarfs and allow us to identify OB stars for follow-up studies. At intermediate colors it would at least identify the sample of stars that must be examined spectroscopically to identify F–G supergiants. The narrowband data would be used to distinguish Hα emission-line stars from planetary nebulae and supernova remnants.

The observing began in 2000 August and ran through 2002 September, with a total of 16 nights of usable data obtained on the CTIO and KPNO 4 m telescopes. Most of this time was spent on M31 and M33, as these spiral galaxies occupied the largest amount of area on the sky (see Figs. 1 and 2). The complete set of images has been available since 2003 via the NOAO Science

Archive[9] and Lowell Web sites.[10] Here we present our *UBVRI* photometry of stars in M31 and M33. Our survey covers 2.2 deg^2 in M31 and 0.8 deg^2 in M33. Subsequent papers will describe the results of our emission-line filters and our broadband photometry of the dwarfs. Our survey has already been used as part of two Ph.D. projects (Williams 2003; Bonanos et al. 2005), as well as other studies (Di Stefano et al. 2004; Massey 2006; Humphreys et al. 2006).

In § 2 we describe our data and go into some detail about the reduction philosophy and technique, since the same methods have been applied to the complete data set. In § 3 we present the catalogs and compare our photometry to that of others. Although spectroscopic follow-up is crucial for addressing many of our science drivers (the dependence of the initial mass function [IMF] and mass upper cutoffs on metallicity and accurate physical H-R diagrams for comparison with stellar evolutionary models), the photometric data alone can be used to good advantage, and we illustrate this in § 4, in which we present color-magnitude diagrams (CMDs) (§ 4.1) and illustrate the power of the photometry in identifying blue and red members (§ 4.2). We test the findings using a preliminary spectroscopic reconnaissance (§ 4.3). We summarize our results and describe our plans for future work in § 5.

---

[9] See http://archive.noao.edu/nsa.
[10] See http://www.lowell.edu/users/massey/lgsurvey.

2. OBSERVATIONS AND DATA REDUCTIONS

In Table 1 we list the field centers and observation dates for all of our M31 and M33 Mosaic frames. The data were taken with the Mosaic CCD camera at the prime focus of the 4 m Mayall telescope. The camera consists of an array of eight thinned 2048×4096 SITe CCDs with 15 μm pixels. The scale is $0''.261$ pixel^{-1} at the center and decreases to $0''.245$ pixel^{-1} at the corners due to pincushion distortion from the optical corrector (Jacoby et al. 1998). To maintain good image quality, an atmospheric dispersion corrector is used during broadband exposures. A single exposure subtends an area of the sky roughly $35' \times 35'$; however, there are gaps between the chips (three gaps of $12''$ each in the north-south direction and one gap of $8''$ east-west), and so the usual observing procedure is to obtain a set of five dithered exposures with the telescope offset slightly ($25''$–$50''$) between each exposure. The area covered by a dither sequence is about $36' \times 36'$.

The basic reductions were performed with the MSCRED package in IRAF.[11] The reductions are somewhat more complicated than that of a normal (single) CCD; complete details can be found at the LGGS Web site. Complications include the fact that there is appreciable cross-talk between pairs of chips that share the same electronics, causing an electronic "reflection" of a small fraction ($\leq 0.3\%$) of the signal of one chip to be added to that of the other. This was most easily seen by the reflection of heavily saturated stars, but if left uncorrected would have affected all of the data on half of the chips. In addition, the corrector introduced a significant ($\leq 10\%$) optical reflection "ghost pupil" of the sky affecting the central portions of the field. Finally, the change of scale resulted in the need to rectify the images using stars with good astrometric positions within the field.

For each run we began by carefully determining the cross-talk terms using the nominal values and revising these until we obtained good subtraction of saturated stars, as judged by eye. Next we constructed a bad-pixel mask by taking the ratio of a series of long and short exposures of the dome flat. This mask would be used to flag nonlinear pixels, which would then not be used in the photometry. For each night we obtained bias frames, dome flats, and sky flats. Given the readout time (130 s), it was not practical to obtain twilight flats in each filter each night, but a good set was obtained on each run. Each set of biases and flats was combined after cross-talk correction and overscan removal. A combination of dome flats and sky flats were needed to construct an image of the ghost pupil for each filter; this ghost was subtracted from the sky flats. After these preliminaries were done, we proceeded as follows: (1) Cross-talk was removed using our revised coefficients. (2) The overscan was removed line by line for each chip, and each chip "trimmed" to remove the overscan region. (3) A revised bad-pixel mask was constructed combining the run-specific image and automatically determining saturated values and any bleed trails. (4) The two-dimensional bias structure was removed by subtracting the average bias frame for the run. (5) The data were flat-fielded using the (cleaned) average sky flats. (6) The filter-specific ghost image was fitted to each image and interactively examined to determine the optimal scaling factor. This correction was most significant for the U and I exposures. (7) An astrometric solution for each frame was performed using stars from the USNO-B1.0 catalog (Monet et al. 2003). The higher order astrometric distortion terms were left at their default values, but individual scales were determined for each axis, as well as rotation. This solution was then used to resample the data (using a time consuming but robust sinc interpolation algorithm),

deprojecting the image to a constant scale ($0''.27$ pixel^{-1}) with conventional astronomical orientation (north up and east left) with a single tangent point for each galaxy. This allowed for simple registration of adjacent fields, if desired.

For many users of the Mosaic camera, the ultimate goal of the basic reduction process is the construction of a single "stacked" image from the processed individual exposures; this image is cosmetically clean, and can then be used for subsequent analysis. We realized at the beginning of the project, however, that this would not be adequate if we were to achieve our goal of 1%–2% photometry through the broadband filters. A simple division of a B and V dome flat suggests that there are highly significant differences in the color terms between the various chips. The stacked image would contain star images that had been combined from as many as four different chips as a result of dithering. Therefore, we made the decision to treat each CCD separately in the photometric analysis. This did require 40 times more work (eight CCDs times five ditherings) in general, but our sense was that in the end we would have significantly better photometry. The stacked images do suffice for the analysis of our narrowband (Hα, [O III], [S II]) data, which we will discuss in future papers.

This decision freed us from the wasteful task of observing broadband standard stars with the 4 m. Since the readout time of the array is 130 s, observing a single standard star offset to each of eight chips through five filters would require nearly 1.5 hr simply in readout time. One could not hope to observe sufficient standards during a night for a precise photometric solution. In addition, the use of external calibration allowed us to make use of nights on the 4 m that were mostly clear but not completely photometric. For the photometric calibration, we used the Hall 1.1 m telescope on Lowell Observatory's dark sky site on Anderson Mesa. Data were obtained on 26 nights from 2000 November through 2003 February. The detector was a 2048×2048 SITe CCD with 24 μm pixels. The chip was binned 2×2, with an image scale of $1''.14$ pixel^{-1} and a field of view of $19'.4 \times 19'.4$. The seeing was typically $2''$–$3''$. For each M31 and M33 field, we obtained two exposures in each filter, with the telescope offset by $500''$ north and $500''$ south of the Mosaic field centers (Table 1). This assured us that there would be overlap between the photometric frames and the area included on each of the Mosaic CCD frames. Exposure times were 1200 s in U, 120 s in each of B, V, and R, and 300 s in I, chosen so there would be good overlap between stars with adequate counts on the calibrating frames and the brightest unsaturated stars on the Mosaic frames. The allocation of observing time on the small telescope was sufficiently generous that we could use only the best, photometric nights. Typically, each calibration field was bracketed by observations of a dozen or so of the best-calibrated (i.e., observed multiple times with errors less than 0.01 mag) Landolt (1992) standards. This allowed us to determine extinction terms accurately; after most of the standard data were reduced, we fixed the values for the color terms and found optimal zero points and extinction values for each night. The average residuals for the standard solutions were 1%–2% for all filters. As usual, we found that the U solutions required two different slopes; one for $U - B > 0$ and one for $U - B < 0$. (See Massey [2002] for discussions of difficulties with calibrating U-band photometry via CCDs and the standard UG2/UG1 + CuSO$_4$ U-like filters.)

For the photometry we developed scripts[12] that separated each of the Mosaic dithered exposures into the eight individual chips,

TABLE 1
Mosaic Observations

Field	$\alpha_{\text{J2000.0}}$	$\delta_{\text{J2000.0}}$	U[a] Date	DIQ (arcsec)	B[b] Date	DIQ (arcsec)	V[b] Date	DIQ (arcsec)	R[c] Date	DIQ (arcsec)	I[d] Date	DIQ (arcsec)
M31-F1	00 47 02.4	+42 18 02	2000 Oct 2	1.2	2000 Oct 2	1.4	2000 Oct 2	1.0	2000 Oct 2	0.9	2000 Oct 2	0.9
M31-F2	00 46 06.5	+42 03 28	2000 Oct 3	1.2	2000 Oct 3	1.1	2000 Oct 3	1.1	2000 Oct 3	0.9	2000 Oct 3	0.9
M31-F3	00 45 10.6	+41 48 54	2000 Oct 6	1.2	2000 Oct 3	1.2	2000 Oct 6	1.1	2000 Oct 6[e]	1.0	2000 Oct 6	1.0
M31-F4	00 44 14.7	+41 34 20	2000 Oct 6	1.1	2000 Oct 6	1.4	2001 Sep 18	1.1	2001 Sep 18	1.1	2001 Oct 6	1.1
M31-F5	00 43 18.8	+41 19 46	2001 Sep 22	1.0	2001 Sep 22	0.9	2001 Sep 22	0.9	2001 Sep 22	0.8	2001 Sep 22	0.8
M31-F6	00 42 22.9	+41 05 12	2002 Sep 11	0.9	2002 Sep 11	0.9	2002 Sep 22	0.9	2002 Sep 22	1.1	2002 Sep 22	1.2
M31-F7	00 41 27.0	+40 50 38	2002 Sep 10	0.9	2002 Sep 10	0.9	2002 Sep 10	0.9	2002 Sep 10	0.8	2002 Sep 10	0.8
M31-F8	00 40 31.1	+40 36 04	2000 Oct 2	1.2	2002 Sep 11	0.9	2000 Oct 2	1.2	2000 Oct 2	1.3	2000 Oct 2	1.1
M31-F9	00 39 35.2	+40 21 30	2000 Oct 3[e]	1.2	2000 Oct 4	1.2	2000 Oct 4	1.1	2000 Oct 4	1.0	2000 Oct 4	1.0
M31-F10	00 38 39.3	+40 06 56	2000 Oct 4	1.1	2000 Oct 4[f]	1.0	2000 Oct 4	1.1	2000 Oct 4	1.0	2000 Oct 4	1.0
M33-North	01 34 00.1	+30 55 37	2001 Sep 18	1.0	2001 Sep 18	1.2	2001 Sep 18	1.2	2001 Sep 18	1.2	2001 Sep 18	0.9
M33-Center	01 33 50.9	+30 39 37	2000 Oct 2/5[g]	1.0	2000 Oct 2/4/5[h]	1.0	2000 Oct 4/5[g]	0.9	2000 Oct 4/5[g]	0.9	2000 Oct 4/5[g]	1.0
M33-South	01 33 11.3	+30 22 10	2001 Sep 18	1.1	2001 Sep 18	1.0	2001 Sep 18	1.0	2001 Sep 18	0.9	2001 Sep 18	0.8

Note.—Units of right ascension are hours, minutes, and seconds, and units of declination are degrees, arcminutes, and arcseconds.

[a] Series of five dithered 600 s exposures unless otherwise noted.
[b] Series of five dithered 60 s exposures unless otherwise noted.
[c] Series of five dithered 50 s exposures unless otherwise noted.
[d] Series of five dithered 150 s exposures unless otherwise noted.
[e] Series of six dithered exposures.
[f] Series of 10 dithered exposures.
[g] Series of six dithered exposures.
[h] Series of 11 dithered exposures.

TABLE 2
COLOR TERMS FOR THE KPNO 4 m MOSAIC CAMERA

	CHIP[b]							
COLOR TERM[a]	1	2	3	4	5	6	7	8
K_{U1}	−0.032	−0.036	−0.033	−0.018	−0.037	−0.031	−0.024	−0.023
K_{U2}	−0.278	−0.260	−0.284	−0.320	−0.260	−0.250	−0.269	−0.243
K_B	−0.145	−0.149	−0.178	−0.148	−0.129	−0.159	−0.155	−0.177
K_V	+0.020	+0.016	+0.008	+0.017	+0.032	+0.021	+0.021	+0.011
K_R	−0.029	−0.059	−0.037	−0.027	−0.016	−0.043	−0.051	−0.037
K_I	+0.042	+0.179	+0.084	+0.110	+0.079	+0.062	+0.007	+0.026

NOTE.—Typical uncertainties in the color terms are 0.005.
[a] The color terms are defined in the text.
[b] Numbered as in the Mosaic manual (Jacoby et al. 2000), starting with the northeastern chip and continuing south along the eastern set of four, and then north along the western four.

and characterized the exposure (median sky value and FWHM) and updated the headers (read noise, saturation value, and gain). Our scripts relied on the basic IRAF DAOPHOT routines (Stetson et al. 1990) but performed the tasks automatically in order to deal with the huge data volumes. Stars $4\,\sigma$ above the local background were found with the appropriate FWHM and image shapes, and aperture photometry was performed with a small (3.5 pixel radius) aperture. This was done independently for each filter. Suitable point-spread function (PSF) stars were automatically identified, and simultaneous PSF fitting was performed over the frame using the ALLSTAR algorithm. Additional stars were added based on residuals from subtracting the fitted PSFs from the original frame, and the simultaneous PSF fitting was repeated. Similar routines were run on the Lowell 1.1 m data, and isolated stars were matched between the data sets to determine photometric zero points and color terms. When all of the data were reduced, we then examined the results and fixed the color terms to the values given in Table 2. The color terms are defined as follows:

$$u_{\mathrm{Mosaic}} = K_{U1}(U-B)_{\mathrm{std}} + C_U, \quad (U-B)_{\mathrm{std}} > 0,$$
$$u_{\mathrm{Mosaic}} = K_{U2}(U-B)_{\mathrm{std}} + C_U, \quad (U-B)_{\mathrm{std}} < 0,$$
$$b_{\mathrm{Mosaic}} = K_B(B-V)_{\mathrm{std}} + C_B,$$
$$v_{\mathrm{Mosaic}} = K_V(B-V)_{\mathrm{std}} + C_V,$$
$$r_{\mathrm{Mosaic}} = K_R(V-R)_{\mathrm{std}} + C_R,$$
$$i_{\mathrm{Mosaic}} = K_I(R-I)_{\mathrm{std}} + C_I,$$

where the K-values are the color terms and the C-values are the zero points. We then reran our calibration program to determine the best zero points.[13]

An examination of the variations of the color terms between chips reveals that our concerns were well founded. Had we treated the chips as identical, we would have introduced a difference of 0.06 mag in U for a lightly reddened O star ($U - B \sim -1$) dithered between chips 4 and 5. Similarly, a RSG ($B - V \sim 2$) would have derived B values that differed by 0.10 mag, depending on whether the star was observed on chip 3 or chip 5. (The derived $B - V$ colors would have been less affected, i.e., a difference of about 0.05 mag.) For projects requiring 5%–10% photometry, or narrowband filters (where color terms are negligible), the use of stacked images should be sufficient, but to be able to achieve 1%–2% broadband photometry (and not be limited by calibration issues) requires some extra work.

We averaged the calibrated photometry for each field, and then compared the differences in adjacent fields, restricting the sample to only well-exposed stars (statistical uncertainty <1%). The results are shown in Table 3. Often the median differences were

---

[13] Note that since the color terms are not the same for each chip, the photometric zero points will not be the same for each chip either, even though they were taken as a single image. The reason is that the flat-field lamps do not have zero color. The error introduced by ignoring this effect would be about 1%–2%. Our calibration procedure explicitly found individual zero points for each chip on each image once the color terms were determined.

TABLE 3
MEDIAN DIFFERENCES OF OVERLAPPING FIELDS

	V		B − V		U − B		V − R		R − I	
FIELDS	No. Stars[a]	Δ[b]	No. Stars[a]	Δ[b]	No. Stars[a]	Δ[b]	No. Stars[a]	Δ[b]	No. Stars[a]	Δ[b]
M31-F1 − M31-F2...................	857	+0.005	441	−0.005	381	−0.013	579	+0.003	623	+0.011
M31-F2 − M31-F3...................	1276	+0.004	692	−0.001	545	+0.004	815	−0.009	904	+0.015
M31-F3 − M31-F4...................	1447	+0.001	772	+0.001	606	+0.003	1124	0.000	1204	−0.009
M31-F4 − M31-F5...................	1524	+0.009	704	−0.009	634	+0.003	928	+0.005	1022	+0.023
M31-F5 − M31-F6...................	1394	−0.003	752	+0.007	713	+0.005	809	0.000	876	−0.017
M31-F6 − M31-F7...................	1624	0.000	817	+0.003	786	+0.007	992	−0.006	1146	−0.035
M31-F7 − M31-F8...................	1431	−0.001	785	+0.006	738	+0.004	892	−0.003	1065	+0.024
M31-F8 − M31-F9...................	1414	−0.002	754	−0.006	676	+0.013	998	−0.004	1144	+0.003
M31-F9 − M31-F10................	992	+0.001	570	+0.001	468	+0.002	821	+0.003	782	−0.002
M33-North − M33-Center	2843	−0.008	1414	+0.004	1720	+0.004	1626	−0.003	2296	+0.010
M33-Center − M33-South	4083	+0.009	2059	−0.010	2422	−0.013	2146	+0.008	3218	−0.026

[a] Number of stars in common with statistical errors ≤0.01 mag in each field.
[b] Median differences (mag).

only several millimagnitudes. Note that this is a critical test of our photometric accuracy, since each field was calibrated independently using external data. We were pleased to find evidence that we generally were able to reduce any calibration issue to <1%, even at U.

Before releasing our final catalogs, we made one additional step, that of removing false detections along diffraction spikes, a problem that has plagued other surveys as well (see, e.g., Magnier et al. 1992). Stars brighter than (roughly) 13 mag had noticeable diffraction spikes, oriented at $45°$ to the cardinal directions. For the brightest foreground stars (7 mag), these diffraction spikes extended ~ 200 pixels from the star. We found that around each bright star there were a handful of false detections in our preliminary catalog. For each source near the coordinates of a bright star, we computed the ellipticity and position angle of the object using the stacked V image for convenience. If the ellipticity was high, and the position angle aligned toward the bright star, we eliminated the source from the catalog. Checking the results visually, we seem to have eliminated nearly all such bogus detections, with little cost in terms of real objects. This affected only 0.1% of the sources in the two catalogs and removed an annoyance.

3. RESULTS

3.1. *The Catalogs*

The final catalog consists of the averaged photometry for each star; of course, many of these stars were observed multiple times (i.e., on five ditherings and possibly on as many as three overlapping fields). For a star to make it into the catalog, it had to be detected in the B, V, and R filters; thus, there are stars without $U - B$ or $R - I$ measurements, and we denote these null measurements with a magnitude of "99.99." The complete M31 and M33 catalogs are available in machine-readable format via the electronic edition of the *Astronomical Journal*; in the printed versions of Tables 4 and 5 we present the first 10 entries of each. The M31 catalog contains a total of 371,781 stars, and the M33 catalog contains a total of 146,622 stars. The stars have been assigned designations based on their celestial (J2000.0) positions; i.e., LGGS J004341.84+411112.0 refers to the star with coordinates $\alpha_{J2000.0} = 00^h43^m41\overset{s}{.}84$, $\delta_{J2000.0} = +41°11'12\overset{''}{.}0$ following IAU conventions. (This particular star is a very close analog of P Cygni and is discussed both in Massey [2006] and below in § 4.3.)

How deep, and complete, is our survey? In terms of the photometric precision, we show the *median* errors as a function of magnitude for the combined M31 and M33 catalogs in Table 6. We see that the errors are <10% through about 23 mag.[14]

Our stated goal was to achieve 1%–2% photometry for massive ($\geq 20 M_\odot$) stars. Did we achieve this? Let us briefly consider the evolution of a $20 M_\odot$ star; for details see Massey (1998a). On the zero-age main sequence the star would be identified as an O9.5 V star and have $M_V = -3.5$. The intrinsic colors of such a star would be $(U - B)_0 \sim -1.1$, $(B - V)_0 \sim -0.3$, $(V - R)_0 \sim -0.1$, and $R - I \sim -0.2$ (Bessell et al. 1998). The observed colors for such a star depend on the reddening; let us assume that the star has an $E(B - V) = 0.25$, typical of several OB associations in M31 (Massey et al. 1986). In that case, we expect such a star to have $U - B = -0.9$, $B - V = 0.0$, $V - R = 0.0$, and

$R - I = 0.0$. Thus, at a distance modulus of 24.4 (M31; van den Bergh 2000), the star would have $U = 20.0$ and $B = V = R = I = 20.9$.[15] The error in R will be slightly larger than our goal (0.027 vs. 0.020 mag), but in all the other bands we will have achieved our goal; for early-type stars it will be UBV that is particularly useful as a temperature discriminant (Massey 1998a). Some 8 million years later, near the end of its hydrogen-burning phase, the star would be a B1 I with $M_V = -5.3$, and nearly identical intrinsic colors, easily within our criteria. Finally, as a He-burning object the star would be spectroscopically identified as a RSG. As an M0 I the star would have $M_V = -6.8$, with intrinsic colors of $(U - B)_0 = 2.5$, $(B - V)_0 = 1.8$, $(V - R)_0 = 0.9$, and $(R - I)_0 = 0.8$, or $U - B = 2.7$, $B - V = 2.0$, $V - R = 1.0$, and $R - I = 1.0$. So, roughly, $U = 22.3$, $B = 19.9$, $V = 17.9$, $R = 16.9$, and $I = 15.9$. The error at U ($\sigma \sim 0.04$) is a little larger than our goal, but the others all give better than 1% statistics. We see in § 4.2 the usefulness of good colors at this magnitude.

However, a more critical test concerns how well we did in crowded regions. Obviously there are stars in M31 and M33 that cannot be resolved from their neighbors; this is true, after all, even for massive stars at 2 kpc distances. But, we were of course curious how well we did in general. In Figure 3 we compare our V stacked LGGS image of OB48, an association rich in massive stars (Massey et al. 1986), with an ACS image shown at the same scale and orientation. We have indicated the stars in our M31 catalog. We see that there are a few cases in which stars were multiple at *HST* resolution but detected as single objects in our survey. But, generally, our ground-based imaging did very well. We call particular attention to the star at left of center in the upper pair. That star is OB48-444, one of the earliest known O stars in M31 (Massey et al. 1995), an O8 I star. Of course, it is possible to have unresolved multiple systems even at *HST* resolution, but as Kudritzki (1998) has emphasized, such multiplicity usually reveals itself by spectral peculiarities.

3.2. *Comparison with Others*

Photometry of galaxy-wide samples of the resolved stellar content of M31 and M33 has mainly been carried out photographically; e.g., Berkhuijsen et al. (1988) for M31 and Humphreys & Sandage (1980) and Ivanov et al. (1993) for M33. Only the Magnier et al. (1992) survey of M31 has used CCDs in such a global study. Others have imaged small areas of these galaxies with CCDs from the ground (e.g., Massey et al. 1986, 1995; Hodge & Lee 1988; Hodge et al. 1988; Wilson et al. 1990), or even smaller regions using *HST* (Hunter et al. 1996a, 1996b; Magnier et al. 1997).

The CCD survey of Magnier et al. (1992) broke new ground by providing *BVRI* photometry of 361,281 stars in a 1 deg^2 area of M31.[16] Indeed, this survey provided much of the inspiration for the present study. We compare the properties of the two surveys in Table 7. Given our larger aperture telescope and the improvement in the size of CCD cameras in the past decade, it is not surprising that our survey goes about 2 mag deeper and covers about twice the area.

---

[14] A few of the very brightest stars have slightly larger errors than some fainter stars. This is due to the fact that the formal errors not only contain the photon and read noise but are also scaled by the reduced χ^2 value of fitting the PSF to a particular star. Since in general the PSF will be based on the average of stars slightly fainter than the brightest star in a frame, the errors of the brighter stars may be higher than expected just based on Poisson statistics.

[15] M33 is another 1/10 mag farther away according to van den Bergh (2000), but the typical reddening of an OB star is less (Massey et al. 1995).

[16] The number of stars in the complete Magnier et al. (1992) catalog is comparable to the number in ours, despite the fact that our survey goes considerably deeper, as we counted as valid only stars that were matched in *B, V, and R* in order to eliminate spurious detections. Stars in Magnier et al. (1992) were usually detected only in a single filter. The number of stars that were detected by Magnier et al. (1992) in *B, V,* and *R* is 19,966, according to their Table 2.

TABLE 4

M31 Catalog

LGGS	$\alpha_{J2000.0}$	$\delta_{J2000.0}$	V	σ_V	$B-V$	σ_{B-V}	$U-B$	σ_{U-B}	$V-R$	σ_{V-R}	$R-I$	σ_{R-I}	N_V	N_B	N_U	N_R	N_I	Sp. Type	Ref.
J003701.92+401233.2..............	00 37 1.92	+40 12 33.2	19.862	0.017	−0.021	0.021	−0.928	0.015	0.204	0.023	99.999	99.999	1	2	1	1	0		
J003701.93+401218.4..............	00 37 1.93	+40 12 18.4	18.739	0.008	1.494	0.015	0.945	0.036	0.946	0.014	99.999	99.999	1	2	1	1	0		
J003702.03+401141.4..............	00 37 2.03	+40 11 41.4	21.225	0.043	1.362	0.085	99.999	99.999	0.748	0.049	0.694	0.024	1	1	0	1	1		
J003702.05+400633.5..............	00 37 2.05	+40 06 33.5	21.091	0.044	0.050	0.061	−1.110	0.052	0.042	0.074	99.999	99.999	1	2	1	1	0		
J003702.13+400945.6..............	00 37 2.13	+40 09 45.6	16.091	0.006	1.287	0.007	0.983	0.007	0.792	0.010	99.999	99.999	1	2	1	1	0		
J003702.24+401225.7..............	00 37 2.24	+40 12 25.7	20.765	0.029	1.584	0.072	99.999	99.999	1.030	0.036	1.262	0.021	1	2	0	1	1		
J003702.38+400529.5..............	00 37 2.38	+40 05 29.5	22.427	0.165	1.359	0.498	99.999	99.999	0.574	0.180	0.892	0.072	1	1	0	1	1		
J003702.44+400723.2..............	00 37 2.44	+40 07 23.2	22.461	0.173	−0.153	0.202	99.999	99.999	−0.018	0.252	99.999	99.999	1	2	0	1	0		
J003702.47+401742.5..............	00 37 2.47	+40 17 42.5	18.026	0.007	1.324	0.011	1.150	0.023	0.732	0.011	0.688	0.008	1	2	1	1	1		
J003702.51+401654.5..............	00 37 2.51	+40 16 54.5	18.768	0.008	0.687	0.012	−0.040	0.014	0.393	0.011	0.390	0.008	1	2	1	1	1		

Notes.—Units of right ascension are hours, minutes, and seconds, and units of declination are degrees, arcminutes, and arcseconds. Table 4 is published in its entirety in the electronic edition of the *Astronomical Journal*. A portion is shown here for guidance regarding its form and content.

References.—For spectral types: (1) Present work; (2) Trundle et al. 2002; (3) Humphreys 1979; (4) Massey et al. 1995; (5) Massey et al. 1986; (6) Humphreys et al. 1990; (7) Bianchi et al. 1994; (8) P. Massey 1996–2006, unpublished; (9) Hubble & Sandage 1953; (10) Humphreys et al. 1988; (11) Massey 1998b; (12) Massey & Johnson 1998 and references therein.

TABLE 5

M33 Catalog

LGGS	$\alpha_{J2000.0}$	$\delta_{J2000.0}$	V	σ_V	$B-V$	σ_{B-V}	$U-B$	σ_{U-B}	$V-R$	σ_{V-R}	$R-I$	σ_{R-I}	N_V	N_B	N_U	N_R	N_I	Sp. Type	Ref.
J013146.16+301855.6..............	01 31 46.16	+30 18 55.6	19.555	0.013	1.533	0.025	1.141	0.047	1.030	0.015	99.999	99.999	1	1	1	1	0		
J013146.18+302932.4..............	01 31 46.18	+30 29 32.4	20.560	0.068	0.645	0.117	99.999	99.999	0.564	0.115	99.999	99.999	1	1	0	1	0		
J013146.18+302931.4..............	01 31 46.18	+30 29 31.4	21.027	0.061	0.090	0.113	0.266	0.118	1.012	0.111	99.999	99.999	1	1	1	1	0		
J013146.20+302706.2..............	01 31 46.20	+30 27 6.2	21.057	0.032	1.857	0.084	99.999	99.999	0.924	0.036	99.999	99.999	1	1	0	1	0		
J013146.21+302026.9..............	01 31 46.21	+30 20 26.9	21.179	0.038	0.962	0.066	0.749	0.096	0.588	0.047	99.999	99.999	1	1	1	1	0		
J013146.25+301849.7..............	01 31 46.25	+30 18 49.7	16.359	0.005	0.811	0.007	0.470	0.007	0.460	0.007	99.999	99.999	1	1	1	1	0		
J013146.26+302931.5..............	01 31 46.26	+30 29 31.5	20.247	0.063	0.912	0.128	0.223	0.131	−0.209	0.112	99.999	99.999	1	1	1	1	0		
J013146.43+302048.4..............	01 31 46.43	+30 20 48.4	21.990	0.074	0.460	0.102	−0.155	0.089	0.308	0.097	99.999	99.999	1	1	1	1	0		
J013146.64+301756.1..............	01 31 46.64	+30 17 56.1	22.075	0.080	1.498	0.156	99.999	99.999	1.121	0.086	99.999	99.999	1	1	0	1	0		
J013146.73+303118.0..............	01 31 46.73	+30 31 18.0	22.110	0.080	1.256	0.153	99.999	99.999	0.710	0.088	0.805	0.037	1	1	0	1	1		

Notes.—Units of right ascension are hours, minutes, and seconds, and units of declination are degrees, arcminutes, and arcseconds. Table 5 is published in its entirety in the electronic edition of the *Astronomical Journal*. A portion is shown here for guidance regarding its form and content.

References.—For spectral types: (1) Humphreys 1980; (2) Massey et al. 1996; (3) Massey et al. 1995; (4) P. Massey 1996–2006, unpublished; (5) Monteverde et al. 1996; (6) Hubble & Sandage 1953; (7) van den Bergh et al. 1975; (8) Massey 1998b; (9) Massey & Johnson 1998 and references therein; (10) Catanzaro et al. 2003.

TABLE 6
MEDIAN ERRORS

Magnitude	σ_U	σ_B	σ_V	σ_R	σ_I
13.0–13.5	0.005	0.005	0.005	0.005	0.001
13.5–14.0	0.005	0.005	0.005	0.005	0.002
14.0–14.5	0.005	0.005	0.005	0.004	0.005
14.5–15.0	0.005	0.024	0.005	0.002	0.005
15.0–15.5	0.005	0.015	0.005	0.002	0.005
15.5–16.0	0.005	0.010	0.005	0.002	0.005
16.0–16.5	0.005	0.002	0.005	0.002	0.004
16.5–17.0	0.005	0.002	0.005	0.002	0.003
17.0–17.5	0.004	0.002	0.005	0.002	0.003
17.5–18.0	0.003	0.002	0.005	0.002	0.002
18.0–18.5	0.004	0.002	0.005	0.003	0.002
18.5–19.0	0.004	0.003	0.005	0.004	0.002
19.0–19.5	0.005	0.004	0.005	0.006	0.002
19.5–20.0	0.006	0.006	0.006	0.008	0.002
20.0–20.5	0.009	0.008	0.009	0.015	0.002
20.5–21.0	0.012	0.012	0.014	0.027	0.002
21.0–21.5	0.018	0.017	0.024	0.038	0.002
21.5–22.0	0.027	0.029	0.044	0.048	0.002
22.0–22.5	0.042	0.054	0.073	0.071	0.013
22.5–23.0	0.079	0.100	0.103	0.153	0.042
23.0–23.5	0.156	0.166	0.255	0.285	0.122
23.5–24.0	0.285	0.265	0.416	0.454	0.234
24.0–24.5	0.420	0.397	0.490	0.491	. . .
24.5–25.0	0.495	0.486	. . .	. . .	. . .

NOTES.—These errors include not only Poisson statistics but also the good-
ness of fit of the PSF. Thus, the errors of some bright stars can be higher than
those of stars somewhat fainter.

We compare our photometry to that of Magnier et al. (1992) in Figure 4. Since the image quality is so different (our worst seeing was their best), we restricted the comparison to stars in our catalog that have no comparably bright companions ($V_{\text{star}} - V_{\text{comp}} < 1$) within $10''$. We have also restricted the comparison to the stars with the best photometry (errors less than 0.05 mag in each filter), although nearly identical values are obtained if we loosen or tighten this restriction. We find median differences (in the sense of Magnier et al. [1992] minus LGGS) of -0.120 in B (5191 stars), -0.025 in V (7214 stars), $+0.019$ in R (4129 stars), and $+0.077$ in I (5387 stars). The differences at V and R are small and as expected; the modest offsets in B and I appear to be real. As shown in the bottom two panels of Figure 4, the reason for the differences at B and I appear to be color related: for the bluest stars, our results and those of Magnier et al. (1992) are in good accord, while for the reddest stars the differences are significantly larger. Stars with $B - V < 0$ show a median difference of -0.025 mag, while stars with $B - V > 1.5$ show a median difference of -0.238 mag. Similarly, there is a strong correlation of the I differences with color, with the bluest stars ($R - I < 0.3$) showing good agreement (median difference -0.024), while the reddest stars ($R - I > 1.2$) show a large difference ($+0.131$). We are of course biased toward believing these color problems are inherent to Magnier et al. (1992) and not our own data, but only independent observations can answer that. We do note that we were careful to include a full range of colors of standards in obtaining our secondary calibration, while Magnier et al. (1992) relied on published M31 photometry for their calibration. At least one of these sources, Massey et al. (1986), was well calibrated for only the bluest stars, and that may help explain some of these differences.

The "DIRECT" BVI CCD surveys of M31 (Mochejska et al. 2001) and M33 (Marci et al. 2001) were aimed at finding eclips-

ing binaries and Cepheid variables to use for improved distances; although they did not cover all of these galaxies, they covered a significantly larger area than those that studied single OB associations. The seeing was relatively poor ($1''.5-1''.8$), but a comparison between their photometry and ours for the brighter stars shows excellent agreement (1%–2%) in all three bandpasses. We are indebted to L. Macri, K. Stanek, and B. Mochejska for communicating these comparisons.

We also were curious to compare our results to the M31 photometry catalog of Berkhuijsen et al. (1988), based on reductions of photographic plates. Massey (2006) noted that there appeared to be a significant magnitude-dependent difference between the V magnitudes of Magnier et al. (1992) and those of Berkhuijsen et al. (1988), at least in a small region around the star AF And. The problem is complicated by the fact that the coordinates in Berkhuijsen et al. (1988) are also known to contain large systematic errors, as noted by Magnier et al. (1992). In comparing their coordinates to ours, we find that we need to correct the Berkhuijsen et al. (1988) coordinates by $-0^{s}.1$ and $+2''.5$ to bring the averages into accord with ours, and that in addition there were problems at the $\pm 5''$ level. The median differences in the photometry are in reasonable agreement: -0.093 in U, -0.046 in B, and -0.040 in V. However, as we can see in Figure 5 there is a very strong effect with magnitude, at V, with the faintest stars in Berkhuijsen et al. (1988) shown in red. Such stars show systematic differences up to several magnitudes! We were concerned that this sort of effect might be due to incorrect matching of stars, given the problems in the Berkhuijsen et al. (1988) coordinates, and so we also made the comparison to just those stars that had both V and B. This is shown in Figure 5 (bottom right). We see the same effect, although of course with fewer data. Since the B data do not show this problem, we conclude that it is not an issue with matching. The problem we find here with the Berkhuijsen et al. (1988) photometry is consistent with Massey (2006), who found a $V = 17.5$ (LGGS) star listed as 18.1 in Berkhuijsen et al. (1988), although the B values agreed well. Not all of the Berkhuijsen et al. (1988) data are affected—there are plenty of fainter stars that do agree with our data—but stars listed as 18 mag or fainter in Berkhuijsen et al. (1988) should be viewed with suspicion. The sort of effect visible in Figure 5 is a classic symptom of problems with sky subtraction, and we were able to confirm that faint stars near the nucleus (where the background is high) show the largest problem.

The only global set of photometry with coordinates that has been published for M33 is that of Ivanov et al. (1993), who present a catalog of blue and red stars based on photographic plates. We find similar problems with those data. We needed to correct the Ivanov et al. (1993) coordinates by $+0^{s}.18$ and $-1''.1$; the match against isolated bright stars in our catalog is usually better than $2''.5$ after this correction. For the "blue supergiants" in their catalog, we find median differences of $+0.22$ mag in U, $+0.04$ mag in B, and -0.08 in V, all based on 558 stars. As we see in Figure 6, the difference in U is primarily a simple offset, while the differences in V are dominated by the faint stars, which show a turndown at the faint end ($V > 19$). This is where we expect errors due to sky determination to be most severe. The red stars show a larger effect, with a median difference of -0.13 mag in B and -0.38 mag in V. (There are no U values for the RSGs in Ivanov et al. [1993].)

Of course, these differences with the photographic studies are not surprising: in their day they represented the best that could be done and provided useful photometry and color information for many years. The advances brought on by improved instrumentation and reduction software result in improved
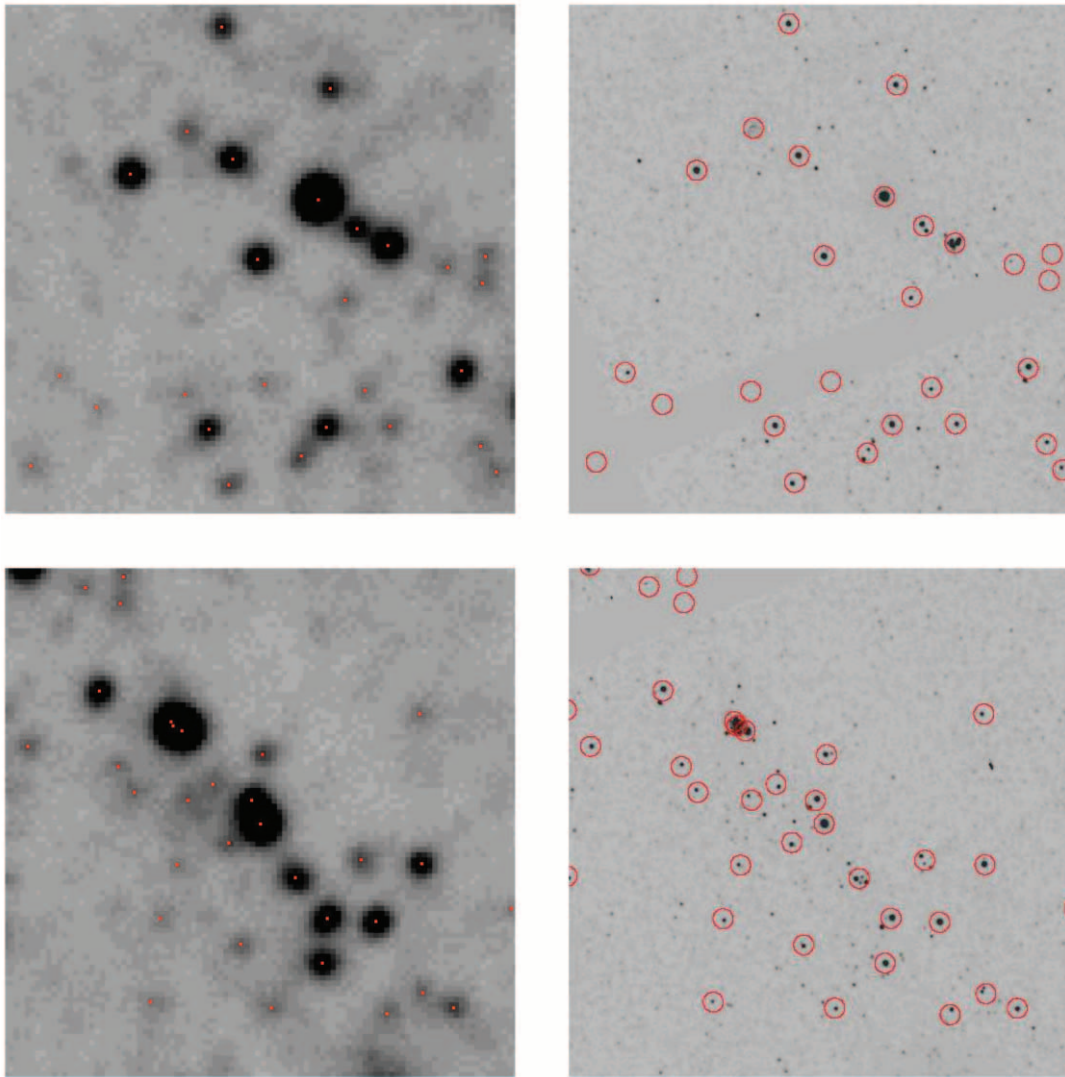
Fig. 3.—Comparison of the LGGS Mosaic field of OB48 with that taken by ACS (F555W filter). The images on the left show a small section of the *V* stacked image of M31-F4 containing OB48, an association rich in massive stars (Massey et al. 1986). The images on the right were obtained with the ACS wide-field camera (F555W filter) on the *HST*, with a scale of 0″.05 pixel^{-1}. We have indicated the stars in our catalog (Table 4). We see that although there are stars that are multiple at *HST* resolution, they are often (but not always!) marked as multiple in our survey as well. Each section is roughly 25″ on a side. The circles on the ACS images have a diameter of 1″.0.

photometry; we hope our study holds up as well over the next two decades.

3.3. *Spectroscopically Confirmed Members*

We considered providing cross-identification between our stars and those of others, particularly Magnier et al. (1992), who

did, after all, provide good coordinates. While this would be meaningful in the less crowded regions, in the OB associations, the exact match depends on whether a given object is identified as one or more stars. This is a particular issue given the large difference in seeing between our survey and that of Magnier et al. (1992). Cross-referencing to Berkhuijsen et al. (1988) is difficult due to the large systematic position errors in that catalog, and probably not useful, given their photometric problems discussed above.

Instead, we decided it would be useful to restrict the cross-identifications to stars spectroscopically confirmed as members of these galaxies. We present these in Tables 8 and 9 and include the spectral types and cross-identifications in Tables 4 and 5 as well. We began with the spectral types given in Massey et al. (1995, 1996), which includes some earlier work (Humphreys et al. 1990), and updated these with more recent data acquired by ourselves and others. Older works, based primarily on photographic spectra, were added to these (e.g., Humphreys 1979, 1980); since these stars lack published coordinates, we did the
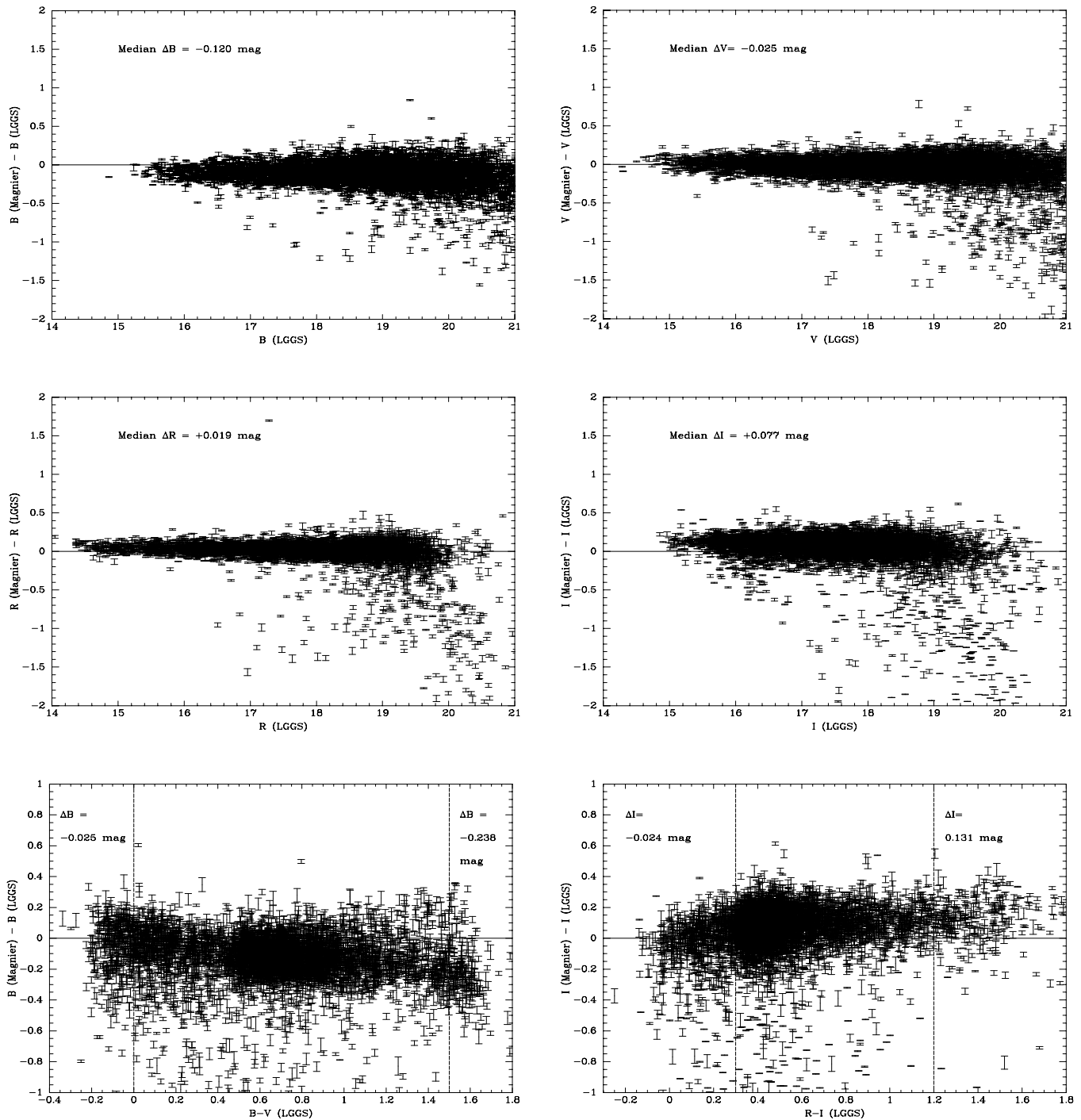
TABLE 7
COMPARISON WITH MAGNIER ET AL. (1992)

Property	LGGS	Magnier et al. (1992)
Filters	*UBVRI*	*BVRI*
Area (deg^2)	2.2	1
Seeing (arcsec)........................	0.8–1.4	1.4–4.0
No. stars[a]...............................	371,781	19,966
5% error	*V* = 22	*V* = 20
PSF fitting	DAOPHOT	DoPHOT

[a] We include here only stars detected in *B*, *V*, and *R*.

FIG. 4.—Comparison between our photometry and that of Magnier et al. (1992) of M31. In making this comparison we have restricted the sample to stars with photometric errors less than 0.05 mag for each filter and stars that are isolated (no significantly bright neighbors within 10″). The median differences are shown. The differences found for *B* and *I* seem to be color related, as shown in the bottom panels.

identifications visually, although we restricted this to alleged members and ignored the wealth of foreground objects such studies tended to confirm. We also included "classical" luminous blue variables (LBVs) from Parker (1997). To this we added recently proposed LBV candidates from King et al. (1998), Massey et al. (1996), and Massey (2006). We included the identifications of Wolf-Rayet stars, drawn from Massey & Johnson (1998). Finally, we included spectroscopically confirmed RSGs, beginning with Massey (1998b) and extending back through Humphreys et al. (1988). For the latter, the membership of some stars is questionable. For instance, Humphrey et al.'s (1988) R79 in M31 is

listed as a "probable supergiant" based on the strength of the Ca II triplet. This star is also known as OB48-416 (Massey et al. 1986); its colors are not those of a RSG but are more like those of an F–G star, and it is likely that the star is a foreground dwarf. Two additional RSG candidates, R138a and R140, fall outside the field covered by our survey. The identification of another RSG candidate, III-R23, was too ambiguous for us to have a positive identification. In general, we concluded that *both* radial velocities and the Ca II triplet strengths are needed to consider a star as a RSG; otherwise, it is listed as a "RSG candidate." The exceptions were stars with demonstrated variability (variable 66
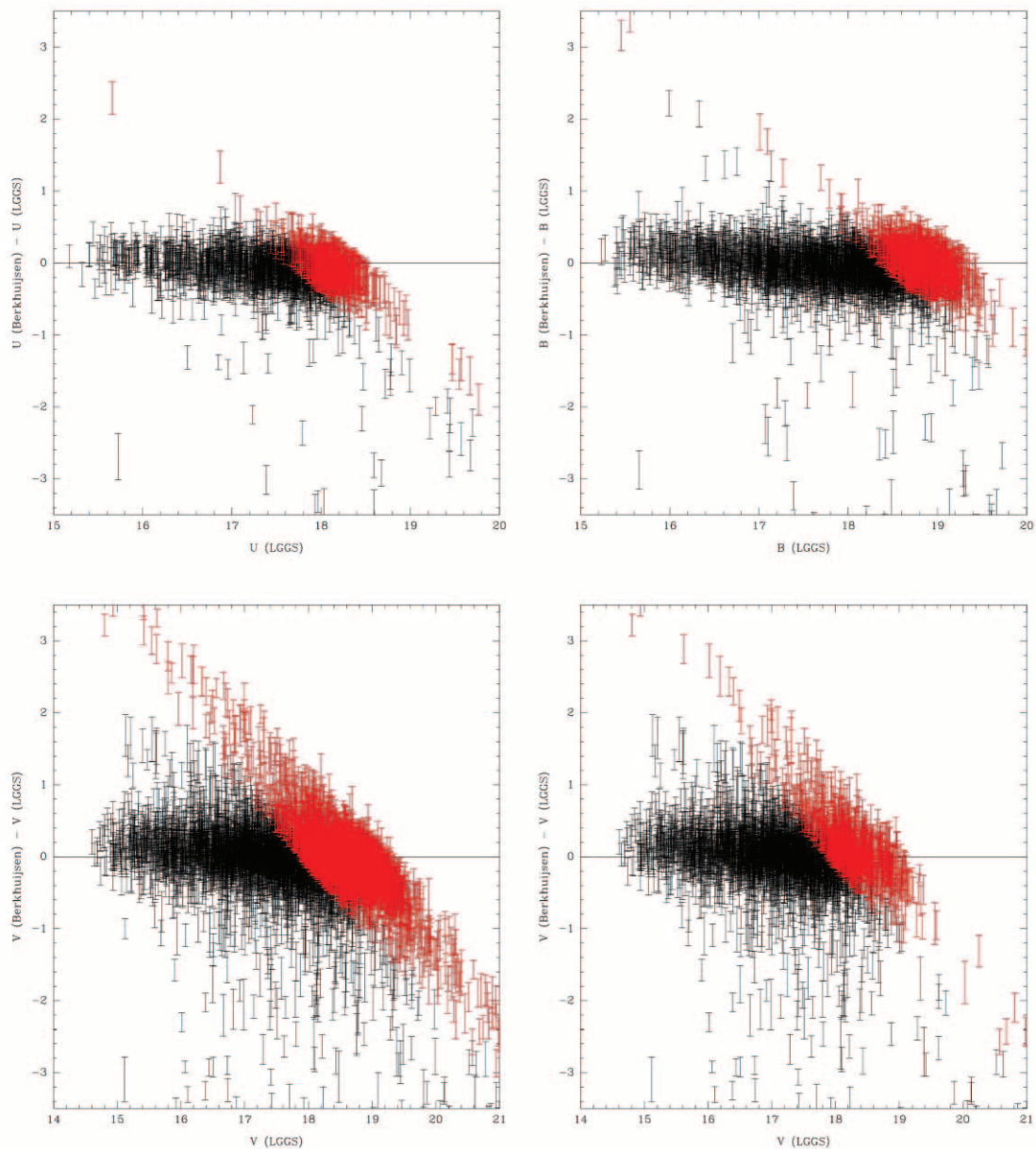
FIG. 5.—Comparison between our photometry and that of Berkhuijsen et al. (1988) of M31. The fainter stars in the Berkhuijsen et al. (1988) catalog are marked in red (for which Berkhuijsen et al. have $U > 17.8$, $B > 18.5$, and $V > 18.0$). The U and B plots show relatively good agreement, but a large systematic effect is present for the fainter stars in V, amounting to several magnitudes. In the plot at bottom right, we make the comparison in V photometry only to those stars that appear in the B comparison. Although fewer data are present, the same trend is evident. Since the same trend is not evident in the B plot, the problem cannot be due to mistaken matches.

from van den Bergh et al. [1975] and variables 4 and 32 from Hubble [1929]).

We also indicate in Tables 8 and 9 whether the object was multiple in our frames. A star is flagged as "M" if it has a companion with $V_{companion} < V_{star} + 2.5$ within $1''$. Multiplicity at this resolution of course calls into question the exact identification; which of two stars separated by a fraction of an arcsecond dominated an optical ground-based spectrum? In some cases the identifications were uncertain because of poor coordinates or finding charts, and we indicate those as well.

In many cases the coordinates are now considerably improved (as for the Moffat & Shara [1983] Wolf-Rayet stars in M31) or, in some cases (such as the spectroscopy of supergiants in field IV of Baade & Swope [1963] by Humphreys [1979], or the spectral types of stars in M33 from Humphreys [1980]), are presented for the first time. In a few instances we went back to our own original finding charts to ascertain whether we had the correct iden-

tifications (e.g., M33WR112, M33WR113, M33WR116, and M33WR117), which had previously only been identified from the poorly reproduced versions of Massey et al. (1987b). The work also showed that two of the RSGs found by Massey (1998b) in M33 had previous spectroscopy by Humphreys (1980). Indeed, it was frustration over such identifications that provided some of the impetus for the present work.

Finally, we also include in Table 8 the newly confirmed M31 members based on the spectroscopy presented in § 4.3 and presented separately in Table 10.

4. ANALYSIS

4.1. Color-Magnitude Diagrams

The most fundamental tool at the astronomer's disposal for understanding the stellar content of a region is the CMD. In Figures 7 and 8 we show the CMDs for M31 and M33, respectively.
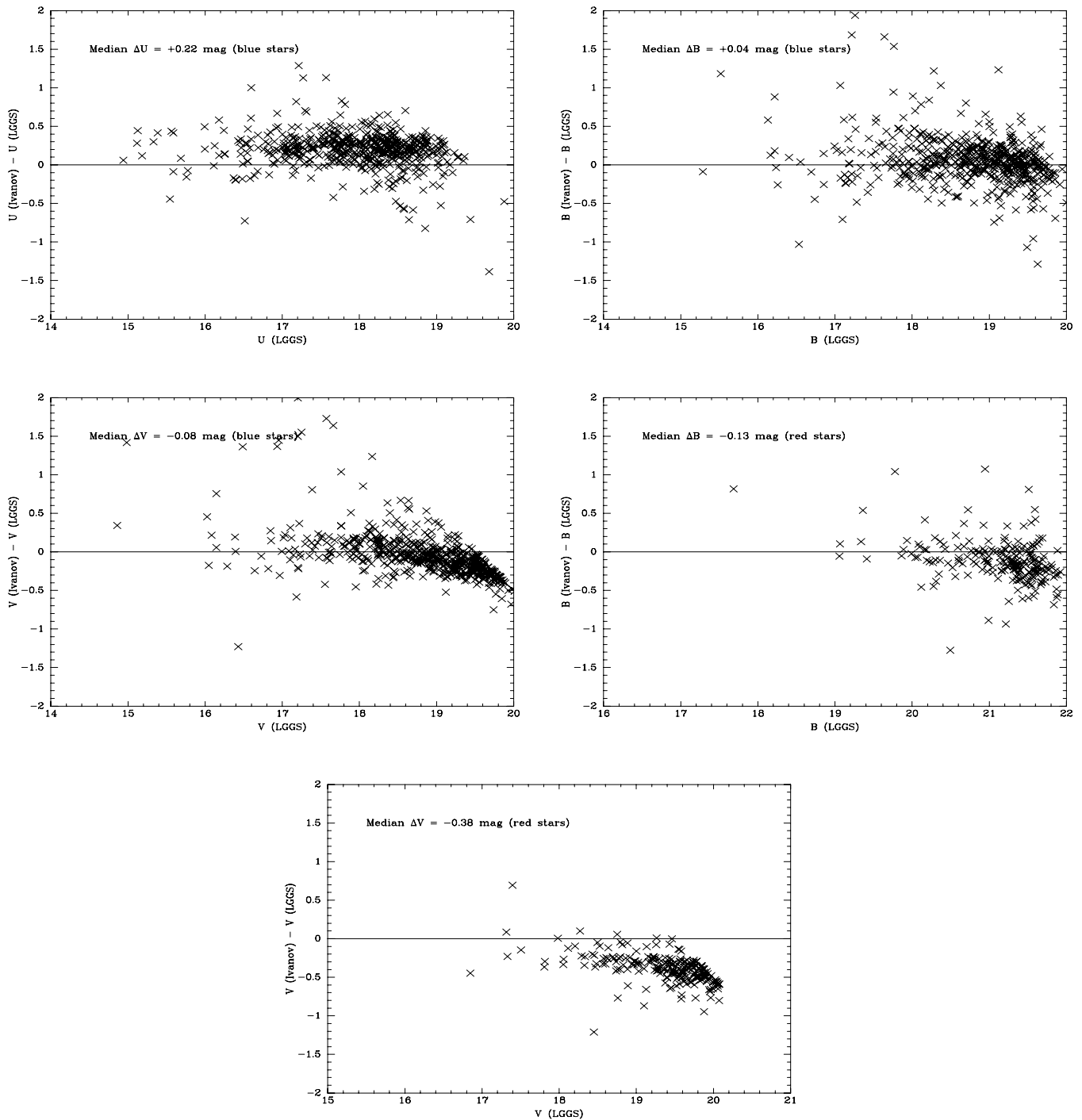
FIG. 6.—Comparison between our photometry and that of Ivanov et al. (1993) of M33. The data for the blue stars show an offset in *U* and a systematic effect with magnitude for *V*. The data for the red stars show systematic problems at the faint end for both *B* and *V*.

We label the regions where we expect to find the blue and red supergiants, as well as the large central region where we expect foreground dwarfs and giants to dominate. The latter is based on a consideration of the Bahcall-Soneira model (Bahcall & Soneira 1980) updated by G. Da Costa and H. Morrison; see Massey (2002). We also show the confirmed members from Tables 8 and 9 with the symbols indicated. There are, of course, fewer foreground dwarfs and giants visible against the face of M33 simply because of the differences in the areas surveyed.

Several things are apparent from these diagrams. First, there is clearly a much more extensive RSG population in M33 than in M31. This effect was first described by van den Bergh (1973),

who noted that the brightest RSGs in low-metallicity galaxies were brighter relative to the brightest blue supergiants than in higher metallicity galaxies. We understand this today as being primarily due to the effects of mass loss on the evolution of massive stars; in high-metallicity regions a 30 $M_\odot$ star will spend little or none of its He-burning life as a RSG, but rather will spend it as a Wolf-Rayet star, while in lower metallicity systems the time spent as a RSG is much longer. (See the discussion in Massey [2002, 2003].)

Second, we see that for M31 we expect few if any of the stars identified as RSGs by Humphreys (1980), which we have labeled as RSG *candidates*, to be actual bona fide RSGs. Instead,

TABLE 8
M31 Members Confirmed by Spectroscopy

LGGS	$\alpha_{J2000.0}$	$\delta_{J2000.0}$	V	$B-V$	$U-B$	$V-R$	$R-I$	Sp. Type	Notes[a]	Cross-ID	Ref.
				O–F Supergiants							
J003728.99+402007.8........	00 37 28.99	+40 20 07.8	17.31	0.11	−0.72	0.06	0.05	B1 I		...	1
J003733.35+400036.6........	00 37 33.35	+40 00 36.6	18.16	−0.21	−0.82	0.21	0.06	B2 Ib–B5 I	M	IV-B59	2
J003734.36+400116.8........	00 37 34.36	+40 01 16.8	18.59	−0.10	−1.12	−0.01	0.00	B0 I		IV-B24	3
J003745.26+395823.6........	00 37 45.26	+39 58 23.6	17.16	0.59	0.27	0.34	0.40	F5 Ia		IV-A207	3
J003751.90+395901.9........	00 37 51.90	+39 59 01.9	18.41	0.08	−0.27	0.07	0.11	A2 Ib		IV-A240	3
J004025.48+404423.6........	00 40 25.48	+40 44 23.6	18.47	−0.12	−1.06	−0.02	−0.04	B0.5 Iab		OB78-63	4
J004028.36+404315.2........	00 40 28.36	+40 43 15.2	18.14	−0.14	−0.86	0.01	−0.77	B0 Ia	M	OB78-159	6
J004028.48+404440.2........	00 40 28.48	+40 44 40.2	17.17	0.02	−0.76	0.08	0.07	B8 I		...	1
J004029.71+404429.8........	00 40 29.71	+40 44 29.8	18.56	−0.23	−1.17	−0.03	0.01	O8.5 I(f)		OB78-231	7
J004030.28+404233.1........	00 40 30.28	+40 42 33.1	17.36	−0.04	−1.13	0.05	0.05	B1.5 Ia	M	OB78-277	7

Notes.—Units of right ascension are hours, minutes, and seconds, and units of declination are degrees, arcminutes, and arcseconds. Table 8 is published in its entirety in the electronic edition of the *Astronomical Journal*. A portion is shown here for guidance regarding its form and content.

[a] (U) Uncertain identification; (M) multiple on a 1″ spatial scale.

References.—For spectral types and cross-identifications: (1) Present work; (2) Trundle et al. 2002; (3) Humphreys 1979; (4) Massey et al. 1995; (5) Massey et al. 1986; (6) Humphreys et al. 1990; (7) Bianchi et al. 1994; (8) P. Massey 1996–2006, unpublished; (9) Hubble & Sandage 1953; (10) Humphreys et al. 1988; (11) Massey 1998b; (12) Massey & Johnson 1998 and references therein.

they are likely to be foreground objects. Two of the "confirmed" RSGs also fall in a peculiar part of the CMD. The brightest of these, J004101.4+410434.6 (OB69-46), has a radial velocity and Ca II triplet line strength consistent with membership, but the $B-V$ color is now 0.4 bluer than the photometry given by Massey (1998b). Possibly the identification of this star has been confused. Four of the RSGs in M33 seem to have a similar problem.

Third, and perhaps the most striking, is that so few of the stars in M31 and M33 have been observed spectroscopically. The characterization of the stellar populations of these galaxies has just begun.

4.2. Identifying the Bluest and Reddest Members from Photometry

One of the complications with identifying the hottest massive stars is the issue of reddening. In the case of M31 and M33 the foreground reddening is small and likely uniform [$E(B-V) = 0.06$ and 0.07, respectively, according to van den Bergh (2000)]; instead, member stars will be reddened by internal absorption within the disks of these galaxies. This adds to some confusion when trying to separate bona fide blue supergiants from foreground dwarfs, a problem apparent in Figures 7 and 8, in which we find some blue supergiants and LBVs intermixed with the foreground stars. (Since this class contains some F supergiants, we do expect some overlap.)

The reddening-free Johnson Q-index[17] provides a useful discriminant of intrinsic color, at least for stars with $Q < -0.6$ (earlier than a B2 V or a B8 I; see Table 3 of Massey 1998c). For instance, consider a star with $B-V = 0.5$ and $V = 18$, a region of the CMD that is heavily dominated by foreground

[17] The quantity $Q = (U-B) - 0.72(B-V)$, where we have adopted the canonical value for the reddening from the Milky Way.

TABLE 9
M33 Members Confirmed by Spectroscopy

LGGS	$\alpha_{J2000.0}$	$\delta_{J2000.0}$	V	$B-V$	$U-B$	$V-R$	$R-I$	Sp. Type	Notes[a]	Cross-ID[b]	Ref.
				O–F Supergiants							
J013233.85+302728.9..............	01 32 33.85	+30 27 28.9	16.44	0.46	0.11	0.24	0.26	F8: I		R354a	1
J013242.92+303847.0..............	01 32 42.92	+30 38 47.0	16.73	0.01	−1.05	0.02	0.06	B2.5 Ia		UIT005	2
J013244.97+303457.7..............	01 32 44.97	+30 34 57.7	17.01	−0.10	−0.86	0.12	0.07	B1.5 Ia	M	UIT007	2
J013250.80+303507.6..............	01 32 50.80	+30 35 07.6	19.94	0.47	−1.05	0.61	0.79	B1: II:		ob21-2	3
J013251.74+303527.6..............	01 32 51.74	+30 35 27.6	18.95	−0.12	−1.12	−0.02	−0.01	Early B?		ob21-8	3
J013252.03+303525.1..............	01 32 52.03	+30 35 25.1	19.21	0.01	−1.03	0.02	0.08	B0.5 Ia		ob21-14	4
J013252.08+303548.7..............	01 32 52.08	+30 35 48.7	19.64	−0.17	−1.15	−0.10	−0.05	B0: I		ob21-16	4
J013252.69+303648.4..............	01 32 52.69	+30 36 48.4	18.45	−0.12	−1.07	−0.05	−0.03	B1: I		UIT015	2
J013255.48+303533.6..............	01 32 55.48	+30 35 33.6	17.99	−0.04	−0.93	0.00	0.04	B5 I		ob21-37	4
J013255.68+303534.7..............	01 32 55.68	+30 35 34.7	17.66	0.02	−0.95	0.08	0.09	B5 Ia		ob21-40	3

Notes.—Units of right ascension are hours, minutes, and seconds, and units of declination are degrees, arcminutes, and arcseconds. Table 9 is published in its entirety in the electronic edition of the *Astronomical Journal*. A portion is shown here for guidance regarding its form and content.

[a] (U) Uncertain identification; (M) multiple on a 1″ spatial scale.

[b] Coordinates substantially improved for M33WR14, M33WR15, M33WR112, M33WR113, M33WR116, and M33WR117.

References.—For spectral types and cross-identifications: (1) Humphreys 1980; (2) Massey et al. 1996; (3) Massey et al. 1995; (4) P. Massey 1996–2006, unpublished; (5) Monteverde et al. 1996; (6) Hubble & Sandage 1953; (7) van den Bergh et al. 1975; (8) Massey 1998b; (9) Massey & Johnson 1998 and references therein; (10) Catanzaro et al. 2003.

TABLE 10
New Spectral Types in M31

LGGS	$\alpha_{J2000.0}$	$\delta_{J2000.0}$	V	$B-V$	$U-B$	$V-R$	$R-I$	Sp. Type	Note[a]
J003728.99+402007.8..............	00 37 28.99	+40 20 07.8	17.31	0.11	−0.72	0.06	0.05	B1 I	
J004028.48+404440.2..............	00 40 28.48	+40 44 40.2	17.17	0.02	−0.76	0.08	0.07	B8 I	
J004032.17+404336.7..............	00 40 32.17	+40 43 36.7	17.69	0.17	−0.67	0.32	0.70	B5 I	
J004032.37+403859.8..............	00 40 32.37	+40 38 59.8	17.76	0.44	−0.70	0.31	0.35	B I	
J004033.80+405717.2..............	00 40 33.80	+40 57 17.2	17.33	0.03	−0.94	0.10	−0.01	B0.2 I + H II	
J004033.90+403047.1..............	00 40 33.90	+40 30 47.1	17.75	0.11	−0.68	0.11	0.12	B I	
J004051.59+403303.0..............	00 40 51.59	+40 33 03.0	16.99	0.22	−0.76	0.22	0.19	LBVCand!	
J004052.19+403116.6..............	00 40 52.19	+40 31 16.6	17.69	0.33	−0.74	0.21	0.23	B8 I	
J004125.29+403438.4..............	00 41 25.29	+40 34 38.4	17.63	0.02	−0.77	0.07	0.11	B5 I	
J004128.67+402324.1..............	00 41 28.67	+40 23 24.1	17.14	−0.19	−1.08	−0.12	−0.16	A V	F
J004204.58+403527.0..............	00 42 04.58	+40 35 27.0	15.56	4.10	99.99	0.49	99.99	G V	F
J004212.27+413527.4..............	00 42 12.27	+41 35 27.4	17.54	0.23	−0.66	0.16	0.17	B2–5 I	
J004246.86+413336.4..............	00 42 46.86	+41 33 36.4	17.79	0.66	−0.41	0.45	0.44	O3–5 If	
J004311.57+414041.1	00 43 11.57	+41 40 41.1	17.49	−0.06	−0.76	0.02	−0.01	B5 I	
J004313.71+414245.3..............	00 43 13.71	+41 42 45.3	17.80	0.12	−0.82	0.09	0.09	Early B I	
J004314.06+415301.8..............	00 43 14.06	+41 53 01.8	17.64	0.02	−0.78	0.06	0.09	B8 I	
J004327.01+412808.7..............	00 43 27.01	+41 28 08.7	17.67	0.22	−0.60	0.39	0.67	B8 I	
J004341.84+411112.0	00 43 41.84	+41 11 12.0	17.55	0.46	−0.76	0.41	0.29	LBVCand	
J004408.97+415511.6..............	00 44 08.97	+41 55 11.6	17.39	−0.13	−1.06	−0.03	−0.02	B0.5 I	
J004412.17+413324.2..............	00 44 12.17	+41 33 24.2	17.33	0.34	−0.65	0.24	0.22	B5: I + H II	
J004416.10+412003.5..............	00 44 16.10	+41 20 03.5	17.73	0.15	−0.74	0.14	0.07	B3 I	
J004422.84+420433.1..............	00 44 22.84	+42 04 33.1	16.46	0.02	−1.02	0.06	0.03	B0.5 I	
J004431.46+415511.0..............	00 44 31.46	+41 55 11.0	17.68	−0.09	−0.99	−0.01	0.06	B1 I	
J004431.65+413612.4..............	00 44 31.65	+41 36 12.4	16.79	0.25	−0.70	0.19	0.14	B2 I	
J004434.65+412503.6..............	00 44 34.65	+41 25 03.6	16.66	−0.05	−0.91	0.04	−0.04	B1: I	
J004438.75+415553.6..............	00 44 38.75	+41 55 53.6	17.25	0.24	−0.86	0.40	0.72	B2 I	
J004440.71+415350.4..............	00 44 40.71	+41 53 50.4	17.25	0.38	−0.55	0.28	0.34	B8 I	
J004441.70+415227.2..............	00 44 41.70	+41 52 27.2	17.34	0.24	−0.60	0.18	0.22	A0 Ie	
J004449.46+412513.6..............	00 44 49.46	+41 25 13.6	17.57	0.19	−0.57	0.16	0.10	B5 I	
J004450.53+412920.0..............	00 44 50.53	+41 29 20.0	17.71	−0.10	−0.91	0.00	−0.02	B1 I	
J004455.13+413133.8..............	00 44 55.13	+41 31 33.8	17.78	−0.08	−1.00	0.01	−0.01	B0.2 I	
J004505.63+413732.3..............	00 45 05.63	+41 37 32.3	17.60	0.00	−0.76	0.03	0.01	B8 I	
J004517.06+413858.5..............	00 45 17.06	+41 38 58.5	17.02	0.13	−0.66	0.13	0.07	B9/A0 I	
J004528.39+414952.7..............	00 45 28.39	+41 49 52.7	16.87	0.09	−0.85	0.10	0.09	B0.2 I	
J004542.10+415601.3..............	00 45 42.10	+41 56 01.3	17.11	0.07	−0.88	0.10	0.03	B1 I	
J004623.14+413847.5..............	00 46 23.14	+41 38 47.5	16.14	0.14	−0.74	0.13	99.99	A0 I	

Note.—Units of right ascension are hours, minutes, and seconds, and units of declination are degrees, arcminutes, and arcseconds.
[a] (F) Foreground star.

dwarfs (Figs. 7 and 8). If $Q = -1.0$ then we can be assured that the star is a reddened early O-type star and a member of M31. If instead its Q-value is -0.4, it could be either an unreddened late F foreground dwarf, or a slightly reddened early A-type supergiant member; without spectroscopy there is no way to tell.

In Figure 9 we show a V versus Q CMD for each galaxy. For M31 there is now cleaner separation between members and nonmembers, as shown by comparing Figure 9 with Figure 7. The results for M33 (Fig. 9 vs. Fig. 8), which has less internal reddening (see Massey et al. 1995), are more ambiguous: the LBVs are now more obvious, but there is still a significant scattering of blue supergiants into redder regions of the diagram. The contrast to M31 is likely due to the fact that simply a lot more stars have spectroscopy in M33, and that some of these stars are quite crowded.

However, Q does not prove very useful for distinguishing among the early-type stars. In Figure 10 we show an expanded region of the plots, where we have color-coded (just) the O–F supergiants by spectral type. In general, the stars of spectral types B5 and later can be distinguished from the O stars, but in neither galaxy is the separation clean. The issue is complicated by crowding (which can affect the photometry and the derived spectral

types) and by the fact that even Q gives only marginally useful separation (see Massey 1998a). The figure illustrates the fact that while the photometry is good at identifying massive stars (as shown by Figs. 7 and 8), quantitative work, such as deriving the IMF, requires follow-up spectroscopy.

Although distinguishing reddened OB stars from foreground dwarfs is only a minor problem, it is virtually impossible to identify RSGs on the basis of a single color. Massey (1998b) found, however, that the two sequences were straightforward (in principle) to separate on the basis of a $B - V$ versus $V - R$ two-color diagram. At a given $V - R$ color, low-surface-gravity stars (supergiants) will have a larger $B - V$ value than will stars with high surface gravities (foreground dwarfs) due to the effects of line blanketing by weak metal lines in the B bandpass. This method should be relatively immune both to reddening and to metallicity; see Figure 1 of Massey (1998b).

We show such two-color diagrams constructed from our catalogs in Figure 11. First we see that there is a very clean separation in the colors, with two easily recognized sequences. Most of the confirmed RSGs indeed fall where we expect in this diagram. A few do not. It would be worth re-examining the membership of the outliers. All of the spectroscopically confirmed nonmembers lie where we expect.
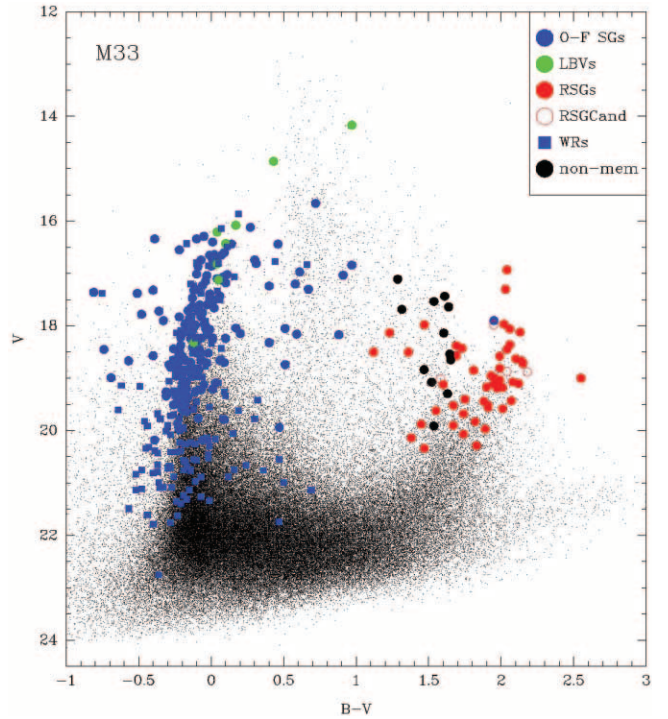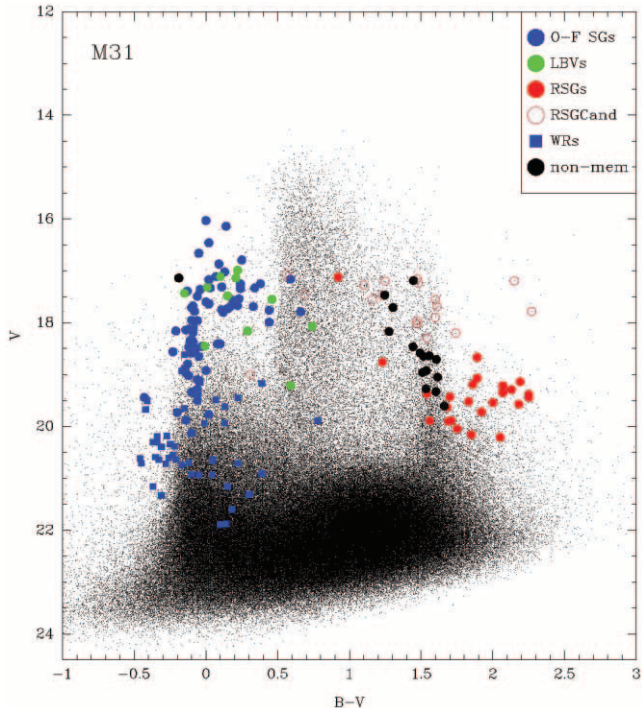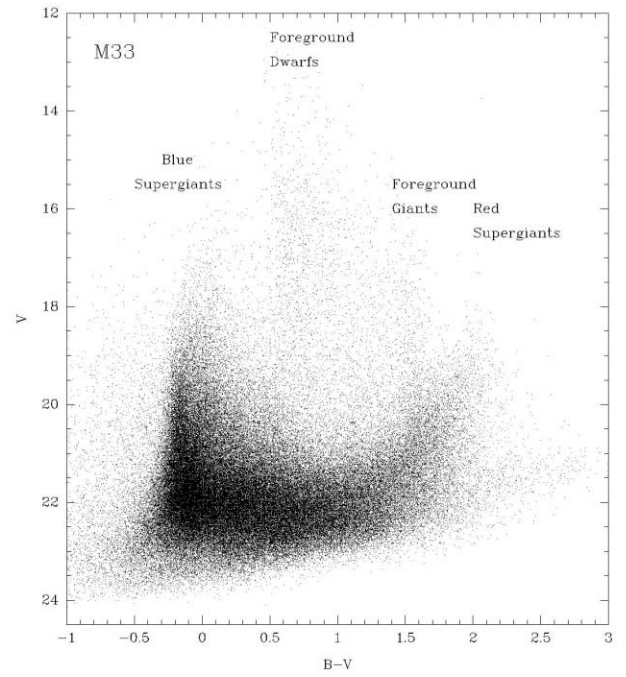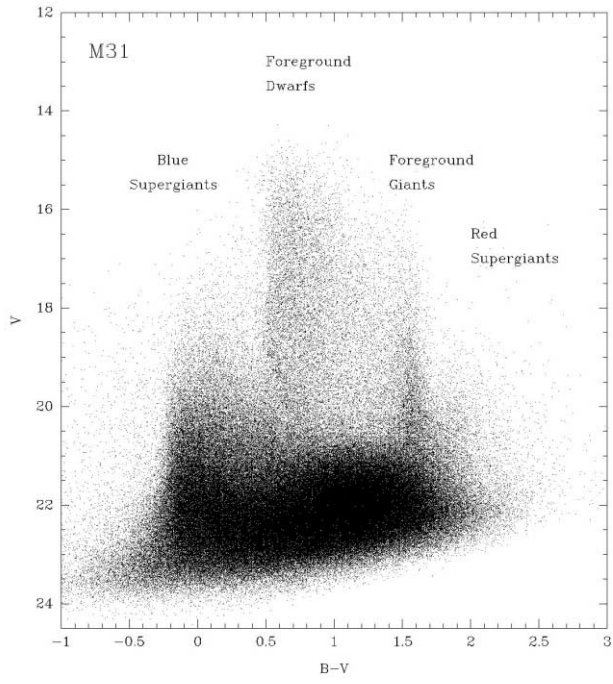
FIG. 7.—CMDs for M31. *Top*: Our interpretation of the major populations. *Bottom*: Confirmed members and nonmembers. The red open circles ("RSGCand") denote candidate RSGs, which may or may not be actual members.

FIG. 8.—CMDs for M33. *Top*: Our interpretation of the major populations. *Bottom*: Spectroscopically confirmed members and nonmembers.
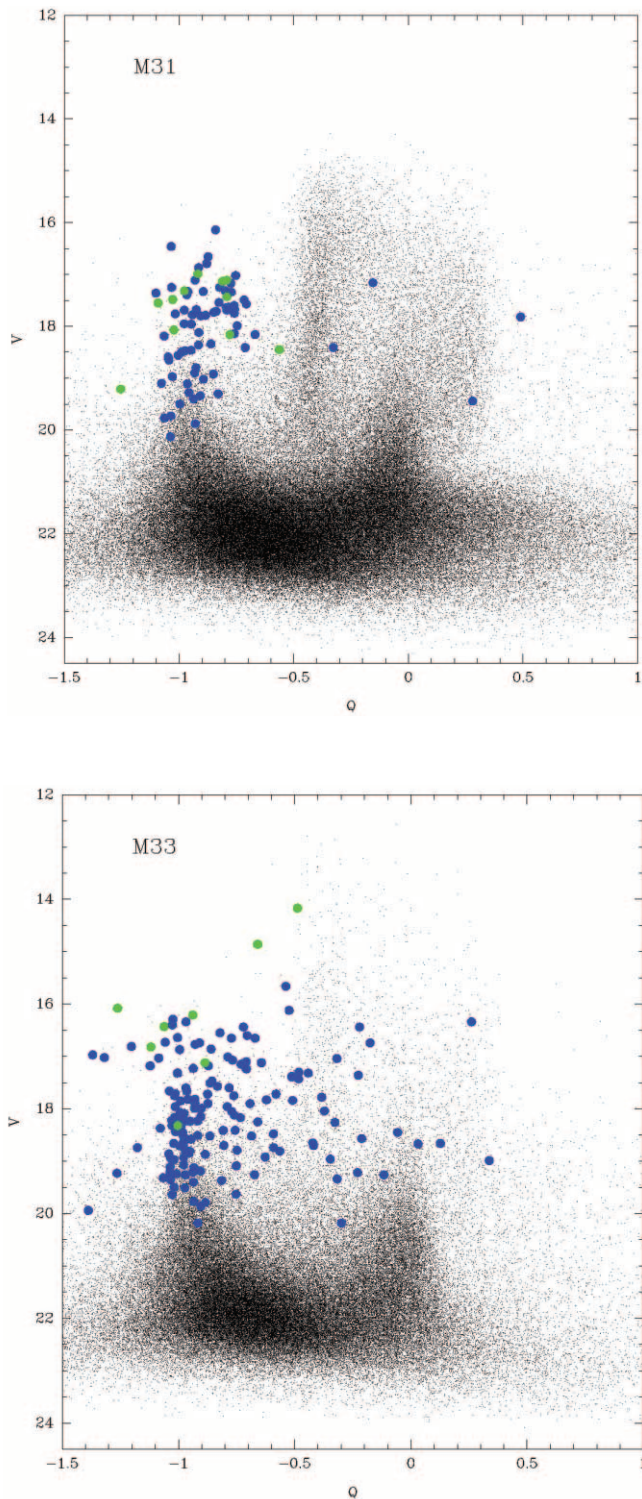
FIG. 9.—Using Q to find blue supergiants. The V magnitudes are plotted against the reddening-free index Q for M31 and M33. We indicate the known O–F supergiants (*blue circles*) and LBVs (*green circles*).

4.3. Illustrations from a Spectroscopic Reconnaissance

Characterizing the stellar populations of these two spiral galaxies to the extent that we can make useful comparisons with the Magellanic Clouds or the Milky Way will require a significant amount of new spectroscopy; with 8 m class telescopes it is now possible to obtain sufficiently high signal-to-noise ratio (S/N) spectra of O and B stars that detailed modeling of the physical

properties can be made. Indeed, such work has already been applied to a few of the brightest B supergiants in these galaxies (see, e.g., Trundle et al. 2002).

However, it is clear from an inspection of Figures 7 and 8 that few of the brightest members have been observed spectroscopically, even to the extent of obtaining crude spectral types or establishing membership or nonmembership. The brightest of these can be usefully surveyed on even 4 m class telescopes, as shown by previous work by Massey et al. (1995) and Humphreys et al. (1990).

On 2005 September 29 we obtained "classification-quality" spectra of the brightest M31 stars using the 3.5 m WIYN telescope[18] and Hydra fiber positioner. The night was photometric, with good seeing ($\leq 1''$). The spectra covered 3970–5030 Å in second order and were obtained with a 790 line mm^{-1} grating (KPC-18C) with a BG-39 blocking filter with a resolution of 1.5 Å. The blue fiber bundle (~ 100 fibers of $3''1$ diameter) was deployed around the $1°$ field of view on targets chosen on the basis of being blue (reddening-free Johnson $Q < -0.6$) and bright ($V < 18$). Two fields were observed: a northern one centered at $\alpha_{J2000.0} = 00^h 44^m 20^s6$, $\delta_{J2000.0} = +41°37'00''$ and a southern one centered at $\alpha_{J2000.0} = 00^h 39^m 45^s7$, $\delta_{J2000.0} = +40°33'00''$. The exposure times were 3 hr on each field, in six 30 minute exposures. Halfway through the sequence the fiber positions were tweaked to take into account changes in the air mass and hence differential refraction. The S/N depended on the star but typically had a value of 50 per 1.5 Å resolution element.

We classified the stars following Walborn & Fitzpatrick (1990). We give these classifications in Table 10. As expected, the vast majority were B supergiants. The O stars, although more luminous, are fainter in V because of their very high effective temperatures and hence significant bolometric corrections. Nevertheless, we do find one Of supergiant, as evidenced by the presence of the characteristic "f" emission signature of N III $\lambda 4634$, 4642 and He II $\lambda 4686$. (The He II emission has an equivalent width of -5 Å, well below the -10 Å cutoff usually assigned for Wolf-Rayet stars; see, e.g., Massey et al. 1987a). The spectrum lacks the S/N needed for an exact classification, but given the weakness of He I, we conclude the star is of spectral type O3–5 If; this makes it *the earliest type O star known in M31*. We show the spectrum in Figure 12. We also give some representative examples of B supergiants in Figure 13. Only two of the spectra we obtained are foreground dwarfs; these are also denoted in Tables 4 and 5.

The most interesting discovery is that of two stars with strong P Cygni profiles. Based on the spectroscopic similarity to P Cygni itself, shown in Figure 14, we consider these two stars as LBV candidates. One of these, J004341.84+411112.0, is the closest known analog to P Cygni and is discussed in more detail in Massey (2006). Photometrically, it has been relatively constant (changing by <0.2 mag) in the optical over the past 40 years, but with small variations (0.05 mag) seen during a single year. Much can be said of the photometric history of P Cygni, which shows only small variability over the same sort of timescale; see Israelian & de Groot (1999). An *HST* image provides circumstantial evidence of a circumstellar nebula, bolstering the case (Massey 2006). The other new LBV candidate, J004051.59+403303.0, is discussed here for the first time. The lines are considerably weaker than in P Cygni; the normalized spectrum has been enhanced by a factor of 4 in Figure 14 to make the lines visible at the scaling needed for the other two. Our photometry indicates $V = 16.99$, $B - V = 0.22$, and $U - B = -0.76$ (all with errors
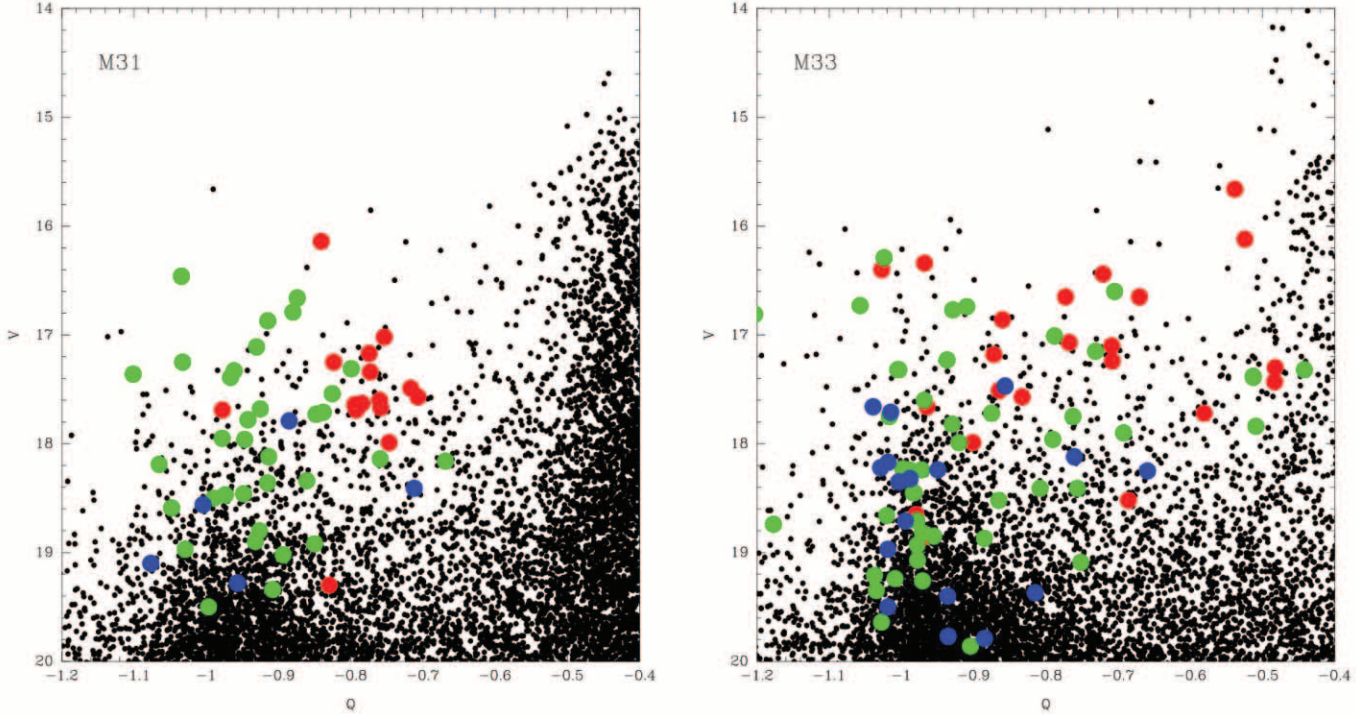

FIG. 10.—Distinguishing among early-type stars based on Q. The V magnitudes are plotted against the reddening-free index Q for M31 and M33. We indicate the known O–F supergiants using colored symbols: O stars (*blue circles*), B0–3 stars (*green circles*), and B5 and later stars (*red circles*).
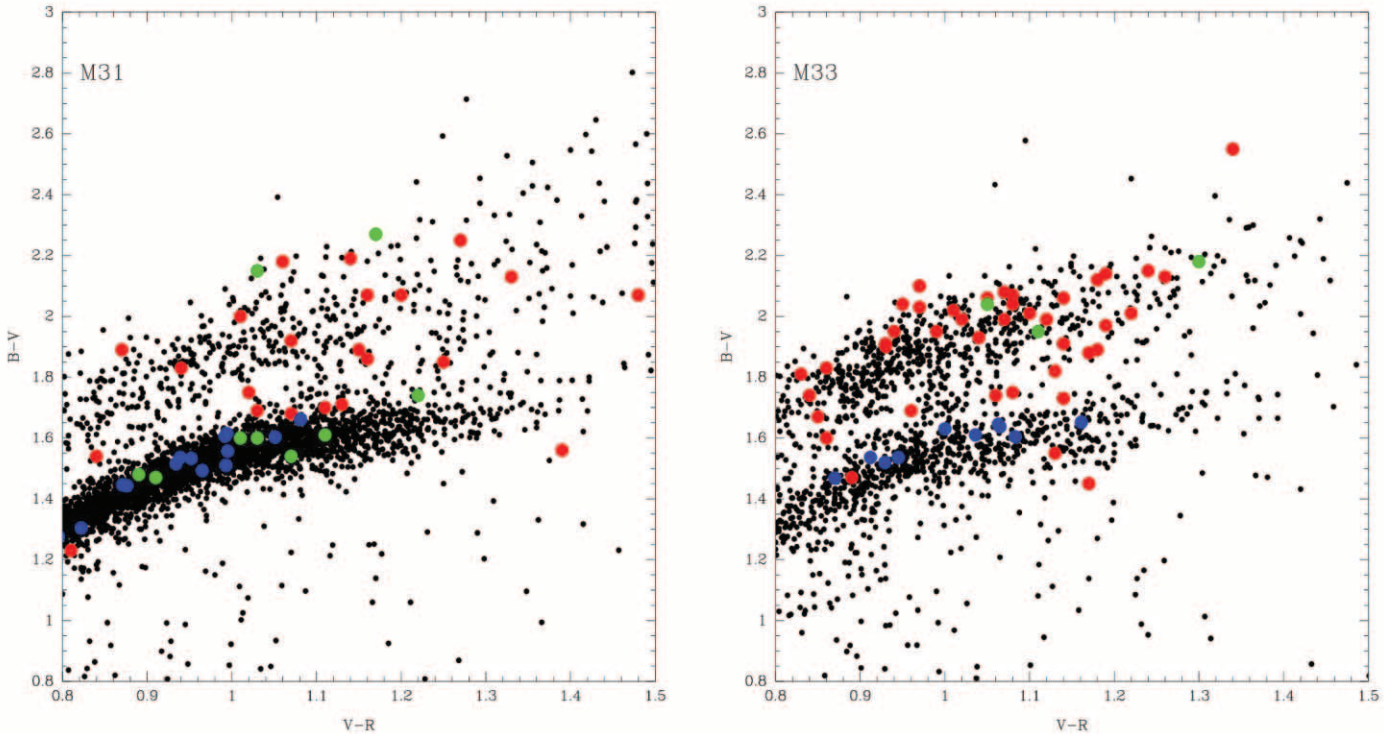

FIG. 11.—Distinguishing RSGs from foreground dwarfs. These $B - V$ vs. $V - R$ plots were made including all stars brighter than $V = 20$. The redder $B - V$ sequence should correspond to RSGs. We show red circles for the spectroscopically confirmed RSGs and blue circles for the stars with spectroscopy that we have called RSG candidates (Tables 8 and 9). The green circles are stars that have been spectroscopically confirmed to be nonmembers.
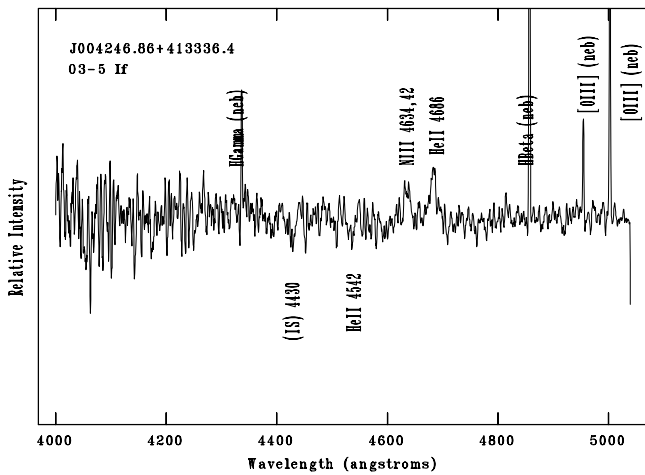
FIG. 12.—O3–5 If star J004246.86+413336.4 in M31. The lack of He I λ4471 relative to the strong He II λ4542 line argues that this star is of early O type (O3–5); the presence of N III λ4634, 4642 and He II λ4686 leads to the "If" designation. This is the earliest O-type star known in M31.
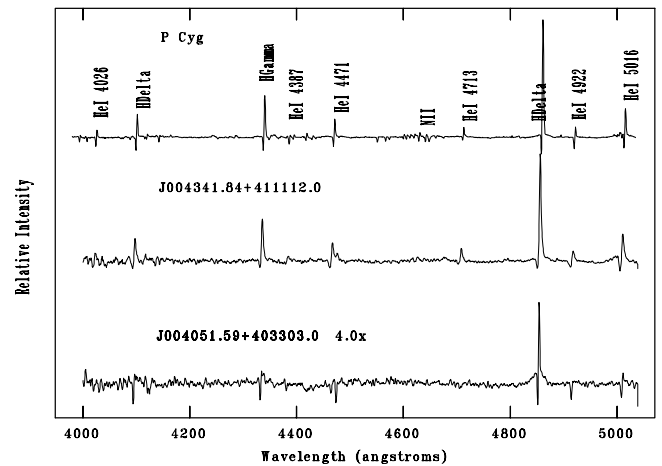
FIG. 14.—Two analogs of P Cygni in M31. Here we compare the spectra of two newly found LBV candidates to that of the archetype LBV Galactic star P Cygni. The scaling of J004051.59+403303.0 has been enhanced by a factor of 4 to make the features visible.

of 0.003 mag) in 2000. Magnier et al. (1992) observed the star in 1990 and found $V = 17.33$ and $B - V = +0.09$, with only slightly larger errors. Thus, this star seems to be a little more variable than the first. The only "proof" that a star is an LBV is for it to undergo a dramatic 1–2 mag "outburst" or show evidence of such a past event in the form of a circumstellar nebula (see Bohannan 1997); in the meantime we must be content to note the spectroscopic similarity to one of the archetypes of LBVs.

5. SUMMARY AND FUTURE WORK

Our *UBVRI* survey of M31 and M33 produced catalogs containing 371,781 and 146,622 stars. We achieved our goal of 1%– 2% photometry for the most massive (>20 $M_\odot$) stars, with the external photometric calibration providing excellent agreement between adjacent fields. Although the image quality of our data is only modest (0″8–1″4, with median 1″0) by modern standards, our survey covered large areas (2.2 and 0.8 deg^2), including all of the regions currently known to be actively forming massive stars. Comparison of our data with an ACS image of OB48, a crowded M31 OB association rich in massive stars, suggests that our catalogs did a respectable job of detecting blends.

Our color-magnitude diagrams demonstrate the rich stellar content of these systems. Although foreground dwarfs and giants will dominate at intermediate colors, most of the stars at either extreme in color will be blue and red supergiants. We demon-

strate this by providing cross-references to stars whose spectroscopy has confirmed their memberships in these systems. New spectroscopy is presented for bright stars in M31, confirming membership for 34 additional members. Among these stars are two newly found LBV candidates, many B–A supergiants, and an O star that is the earliest type known in that galaxy.

Future work is needed to avail ourselves of these beautiful data. Only a tiny fraction of these stars have been observed spectroscopically. Follow-up spectroscopic surveys on larger telescopes will allow us to determine the initial mass functions for numerous regions of star formation, and help determine if and how the IMF varies with metallicity and other conditions. High-S/N spectra can be used to model a range of spectral types, helping to establish how metallicity affects fundamental stellar properties such as effective temperature. In addition, our team will continue to analyze our existing data on other Local Group galaxies currently actively forming stars and compare those CMDs to those presented here.

The premise of the NOAO Survey Program was that data such as those presented here should be useful to others for their own research. Toward that end we have made our full catalogs and images available; in addition, we have carefully documented our reduction techniques and have also made our software available.
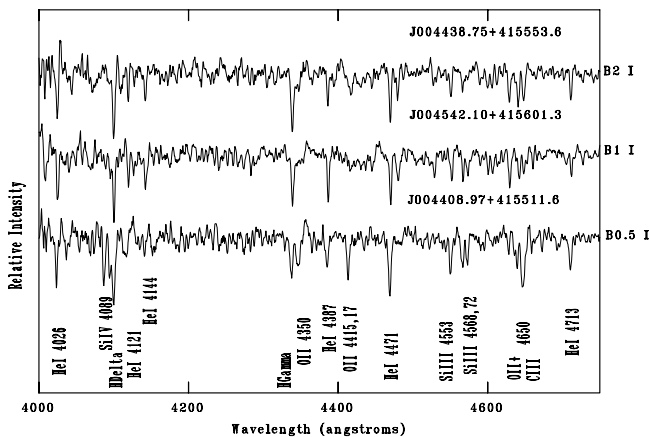

FIG. 13.—Three early B supergiants in M31. The principal lines are identified.

REFERENCES

Baade, W., & Swope, H. H. 1963, AJ, 68, 435
Bahcall, J. N., & Soneira, R. M. 1980, ApJS, 44, 73
Berkhuijsen, E. M., Humphreys, R. M., Ghigo, F. D., & Zumach, W. 1988, A&A, 192, 299
Bessell, M. S., Castelli, F., & Plez, B. 1998, A&A, 333, 231
Bianchi, L., Lamers, H. J. G. L. M., Hutchings, J. B., Massey, P., Kudritzki, R., Herero, A., & Lennon, D. J. 1994, A&A, 292, 213
Bohannan, B. 1997, in ASP Conf. Ser. 120, Luminous Blue Variables: Massive Stars in Transition, ed. A. Nota & H. J. G. L. M. Lamers (San Francisco: ASP), 3
Bonanos, A. Z., et al. 2005, BAAS, 207, 104.07
Catanzaro, G., Bianchi, L., Scuderi, S., & Manchado, A. 2003, A&A, 403, 111
Di Stefano, R., et al. 2004, ApJ, 610, 247
Hodge, P., & Lee, M. G. 1988, ApJ, 329, 651
Hodge, P., Lee, M. G., & Mateo, M. 1988, ApJ, 324, 172
Hubble, E. 1929, ApJ, 69, 103
Hubble, E., & Sandage, A. 1953, ApJ, 118, 353
Humphreys, R. M. 1979, ApJ, 234, 854
———. 1980, ApJ, 241, 587
Humphreys, R. M., Massey, P., & Freedman, W. L. 1990, AJ, 99, 84
Humphreys, R. M., Pennington, R. L., Jones, T. J., & Ghigo, F. D. 1988, AJ, 96, 1884
Humphreys, R. M., & Sandage, A. 1980, ApJS, 44, 319
Humphreys, R. M., et al. 2006, AJ, submitted
Hunter, D. A., Baum, W. A., O'Neil, E. J., Jr., & Lynds, R. 1996a, ApJ, 456, 174
———. 1996b, ApJ, 468, 633
Israelian, G., & de Groot, M. 1999, Space Sci. Rev., 90, 493
Ivanov, G. R., Freedman, W. L., & Madore, B. F. 1993, ApJS, 89, 85
Jacoby, G. H., Liang, M., Vaughnn, D., Reed, R., & Armandroff, T. 1998, Proc. SPIE, 3355, 721
Jacoby, G. H., et al. 2000, NOAO CCD Mosaic Imager User Manual (KPNO System; Tucson: NOAO)
King, N. L., Walterbos, R. A. M., & Braun, R. 1998, ApJ, 507, 210
Kudritzki, R. P. 1998, in Stellar Astrophysics for the Local Group, ed. A. Aparicio, A. Herrero, & F. Sanchez (Cambridge: Cambridge Univ. Press), 149
Landolt, A. U. 1992, AJ, 104, 340
Magnier, E. A., Hodge, P., Battinelli, P., Lewin, W. H. G., & van Paradijs, J. 1997, MNRAS, 292, 490
Magnier, E. A., Lewin, W. H. G., van Paradijs, J., Hasinger, G., Jain, A., Pietsch, W., & Trümper, J. 1992, A&AS, 96, 379

Marci, L. M., Stanek, K. Z., Sasselov, D. D., Krochenberger, M., & Kaluzny, J. 2001, AJ, 121, 861
Massey, P. 1998a, in ASP Conf. Ser. 142, The Stellar Initial Mass Function, ed. G. Gilmore & D. Howell (San Francisco: ASP), 17
———. 1998b, ApJ, 501, 153
———. 1998c, in Stellar Astrophysics for the Local Group, ed. A. Aparicio, A. Herrero, & F. Sanchez (Cambridge: Cambridge Univ. Press), 95
———. 2002, ApJS, 141, 81
———. 2003, ARA&A, 41, 15
———. 2006, ApJ, 638, L93
Massey, P., Armandroff, T. E., & Conti, P. S. 1986, AJ, 92, 1303
Massey, P., Armandroff, T. E., Pyke, R., Kanan, P., & Wilson, C. D. 1995, AJ, 110, 2715
Massey, P., Bianchi, L., Hutchings, J. B., & Stecher, T. P. 1996, ApJ, 469, 629
Massey, P., Conti, P. S., & Armandroff, T. E. 1987a, AJ, 94, 1538
Massey, P., Conti, P. S., Moffatt, A. F. J., & Shara, M. M. 1987b, PASP, 99, 816
Massey, P., & Johnson, O. 1998, ApJ, 505, 793
Meynet, G., & Maeder, A. 2005, A&A, 429, 581
Mochejska, B. J., Kaluzny, J., Stanek, K. Z., & Sasselov, D. D. 2001, AJ, 122, 1383
Moffat, A. F. J., & Shara, M. M. 1983, ApJ, 273, 544
Monet, D. G., et al. 2003, AJ, 125, 984
Monteverde, M. I., Herrero, A., Lennon, D. J., & Kudritzki, R. P. 1996, A&A, 312, 24
Parker, J. W. 1997, in ASP Conf. Ser. 120, Luminous Blue Variables: Massive Stars in Transition, ed. A. Nota & H. Lamers (San Francisco: ASP), 368
Stetson, P. B., Davis, L. E., & Crabtree, D. R. 1990, in ASP Conf. Ser. 8, CCDs in Astronomy, ed. G. H. Jacoby (San Francisco: ASP), 289
Trundle, C., Dufton, P. L., Lennon, D. J., Smartt, S. J., & Urbaneja, M. A. 2002, A&A, 395, 519
van den Bergh, S. 1964, ApJS, 9, 65
———. 1973, ApJ, 183, L123
———. 2000, The Galaxies of the Local Group (Cambridge: Cambridge Univ. Press)
van den Bergh, S., Herbst, E., & Kowal, C. T. 1975, ApJS, 29, 303
Walborn, N. R., & Fitzpatrick, E. L. 1990, PASP, 102, 379
Williams, B. F. 2003, AJ, 126, 1312
Wilson, C. D., Madore, B. F., & Freedman, W. L. 1990, AJ, 99, 149